Different Condition Monitoring Approaches for Main Shafts of Offshore Wind Turbines

Ambühl, Simon; Sørensen, John Dalsgaard

Publication date:
2016

Document Version
Publisher's PDF, also known as Version of record

Aalborg University
Department of Civil Engineering
Reliability and Risk Analysis Research Group

DCE Technical Report No. 212

Different Condition Monitoring Approaches for Main Shafts of Offshore Wind Turbines

by

Simon Ambühl
John Dalsgaard Sørensen

October 2016

Scientific Publications at the Department of Civil Engineering

Technical Reports are published for timely dissemination of research results and scientific work carried out at the Department of Civil Engineering (DCE) at Aalborg University. This medium allows publication of more detailed explanations and results than typically allowed in scientific journals.

Technical Memoranda are produced to enable the preliminary dissemination of scientific work by the personnel of the DCE where such release is deemed to be appropriate. Documents of this kind may be incomplete or temporary versions of papersor part of continuing work. This should be kept in mind when references are given to publications of this kind.

Contract Reports are produced to report scientific work carried out under contract. Publications of this kind contain confidential matter and are reserved for the sponsors and the DCE. Therefore, Contract Reports are generally not available for public circulation.

Lecture Notes contain material produced by the lecturers at the DCE for educational purposes. This may be scientific notes, lecture books, example problems or manuals for laboratory work, or computer programs developed at the DCE.

Theses are monograms or collections of papers published to report the scientific work carried out at the DCE to obtain a degree as either PhD or Doctor of Technology. The thesis is publicly available after the defence of the degree.

Latest News is published to enable rapid communication of information about scientific work carried out at the DCE. This includes the status of research projects, developments in the laboratories, information about collaborative work and recent research results.

Published 2016 by
Aalborg University
Department of Civil Engineering
Thomas Manns Vej 23
DK-9220 Aalborg Ø, Denmark

Printed in Aalborg at Aalborg University

ISSN 1901-726X
DCE Technical Report No. 212

Abstract

Condition monitoring can be used to detect faults and failures at an early stage. Thus it decreases the overall maintenance expenses. This report gives an example of condition monitoring with focus on early crack detection in the main shaft of an offshore wind turbine. This article discusses the applicability of different condition monitoring techniques like performance monitoring, strain gauge results and vibration analysis for crack detection on the low speed shaft. Different signal processing methods like descriptive statistics, Fourier Transforms, Wavelet transforms, Modal Assurance Criteria and Time Synchronous Averaging are investigated and tested for applicability in order to detect cracks on the low speed shaft of a wind turbine. The results of this study can be used to define alarm thresholds as well as detection characteristics for main shaft cracks leading to failure of the main shaft. The example in this paper showed that the crack on the main shafts needs to be relatively large (around 20 $\%$ of the main shaft diameter) until it can be detected.

Acknowledgements

The authors wish to thank the financial support from the Danish Council for Strategic Research (Contract $10-093966$, REWIND: Knowledge based engineering for improved reliability of critical wind turbine components) which made this work possible.

Contents

Chapter 1

Introduction

Wind technology is a fast growing market for renewable electricity production. In 2014, a total wind power capacity of 51 GW was installed and reached 370 GW [45] by the end of 2015. Trends show (Europe: [20]; Worldwide: [28]) that the installed offshore wind capacity is expected to strongly grow in the future. In 2014, 12.6% [20] of the total new installed wind power capacity were erected offshore, reaching a total offshore installed wind power capacity of 8045.3 MW by the end of 2014 producing 29.6 TWh in 2014 [28].
Wind turbines are unmanned power plants which are exposed to highly variable and harsh weather conditions. These varying weather conditions lead to highly variable operational conditions which make maintenance necessary. Maintenance costs, which contain all costs necessary during the life time of a machine in order to keep the machine in service, are important cost drivers for offshore wind turbines. For offshore wind turbines, the operation and maintenance costs to the total cost of energy are typically in the order of 25% [23] of the levelized cost of energy.
Therefore, large efforts are in progress in order to decrease the overall maintenance costs especially for offshore wind turbines. One possibility to decrease operation and maintenance expenses is the possibility to better plan maintenance actions. In order to better plan maintenance actions (inspections) for offshore wind turbines, it is beneficial to observe the condition of important structural parts in order to have knowledge about the condition of the components before accessing the wind turbine. This condition-based preventive maintenance, which is according to [2] the most modern and popular maintenance strategy, is discussed in the literature. Access to the wind turbines offshore is expensive due to limited access times (no access possible during storms) as well as long transportation times and expensive equipment (e.g. special cranes/ships needed). Condition monitoring can be used to record the condition of a certain structural component and to detect possible failures before they occur. Condition monitoring can be performed by either installing special condition monitoring systems (like e.g. vibration sensors) or by SCADA (Supervisory control and data acquisition) variable observation over time where unusual changes of these variables in time can indicate a future failure of a wind turbine component. A combination of both systems makes it possible to reduce false alarms displayed by the SCADA system when carrying out a detailed investigation of the true failure caused by condition monitoring systems compared with merely measured amplitudes, which are used for triggering fault alarm [57, 60].
Condition monitoring for static objects like dams or bridges is generally called structural health monitoring (SHM) in literature. Based upon the common use of the words *condition monitoring* and *structural health monitoring*, condition monitoring focuses more on machines (or machine parts) whereas structural health monitoring deals with the state of the structural components. Fault diagnostic systems, which are part of the condition monitoring system, are commonly used in aircraft and power station turbines where vibration measurements are state of the art [25]. Furthermore, also in the paper industry, the railway industry and for crane applications as well as industry robots damage, prevention measures are used to perform condition monitoring [19]. Especially on rotating structures condition monitoring is important due to cyclic loading and fatigue behavior.
Preventive maintenance is of importance for offshore wind turbines (OWTs) due to the fact that in case of failure, long waiting times may occur and the transportation/installation costs are high. For OWT components, condition maintenance has mainly be applied to parts with relatively high failure rates like bearings, gearboxes, generators, and power electronics as well as components made out of composites like the blades. Condition monitoring of the main shaft is of importance as a broken main shaft will lead to large secondary damages and is expensive to be replaced even though the failure probability is small. According to [53, 9] between 1% and 4% of all failures are located at the main shaft. Replacement of a broken main shaft for a 2 MW turbine costs 50% [19] of the initial investment costs of an entirely new wind turbine plus additional costs due to secondary damages as well as loss of electricity production. Detailed reviews about already used condition monitoring methods for different com-

ponents mounted on a wind turbine are given e.g. in [25, 36, 57, 51, 6, 37, 4, 14] or for reviews about condition monitoring technologies in general, see e.g. [47, 30].
Condition monitoring is, in general, divided into six different steps [38] as shown in Figure 1.1. The first step of a condition monitoring process consists of data acquisition where a physical phenomenon is transferred into a measurable parameter. Then the data (measurements) of this parameter needs to be processed in order to conclude on the component health. In a third step, the processed data enables indication of normal or abnormal conditions. If the condition is normal, no further actions need to be performed. When the condition is detected as abnormal, validation of the fault as well as its location and severity need to be determined. Based on the outcome of the diagnosis, an estimation on how long the faulty component will last until it fails is performed i.e. the remaining useful life (RUL). In the last step, recommendations from the prognosis are given stating what maintenance actions should be performed at which time.
This paper focuses on condition monitoring studies related to cracks on the low speed shaft of a wind turbine.

Figure 1.1: Different steps to be included in condition monitoring.

Different condition monitoring methods are tested and their applicability for failure detection at the low speed shaft are investigated. The outcome of this study can be used as starting point for low speed shaft condition monitoring implementations in wind turbines. The analysis is based on simulated data from FAST [32] but takes the randomness of the environmental conditions like turbulence intensity and crack modeling into account.

Chapter 2

Condition Monitoring Techniques for Wind Turbine Drivetrains

Condition monitoring converts a physical measurement (e.g. vibrations or temperatures) at a certain position in the machine into recommendations for actions. This method allows scheduling of maintenance or other actions in order to minimize the consequences of failure before it occurs. Therefore, changes in the machinery conditions need to be detected on time and the detection method itself should be reliable. The gained knowledge is used for future developments in order to mitigate measures. Condition monitoring is not applicable for avoiding sudden failures, but enables decreasing of the overall maintenance costs by observation and early detection actions [56]. Symptoms which may indicate a crack or initiate failure of a structural component of the drivetrain are e.g. [48]:

- Elevated vibrations (due to e.g. unbalanced blades, mechanical looseness, resonance problems or gear damage)
- Increased noise levels (due to e.g. gear damage, misalignments, mechanical looseness or resonance problems)
- Oil contamination (due to e.g. inadequate lubrication conditions or gear damage)
- Overheating (due to e.g. inadequate lubrication systems, generator problems or misalignments)
- Component performance degradation (e.g. due to electrical problems or bearing problems)

The time history response of a structural component or system can be measured by a variety of sensors. In addition, the following condition monitoring techniques can be considered in order to monitor the above mentioned symptoms [54, 25, 39, 57, 14]:

- Vibration analysis
- Acoustic measurements
- Oil monitoring
- Thermography
- Strain gauges
- Ultrasonic techniques
- Shock pulse method
- Process parameter or component performance monitoring
- Visual inspection (cameras)
- Electrical effects

The obtained signals can be processed in different ways like [11, 30, 57, 6, 14]:

- Amplitude demodulation (resolving periodic events with low amplitude/frequency)

- Frequency domain analysis (Fourier Transformation, Wavelet Transformation, Time Synchronous Averaging, Modal Assurance Criteria, Cepstrum analysis)
- Time-domain analysis (Time Synchronous Averaging, Descriptive statistics)
- Hidden Markov models
- Filtering methods
- Trend analysis
- Other (novel) approaches

The analysis algorithms for condition monitoring can either work in the time domain or in the frequency domain. In the time domain, extreme values within a certain time range, the mean value as well as its scattering could be analyzed whereas in the frequency domain side band analyzes or envelope analyzes could be performed in order to identify possible abnormalities of the component and future structural failures. Spectrum analyzes can be performed for a certain frequency as well as on the overall spectrum. In wind turbine farms, the results can also be compared with neighboring turbines in order to gain more information [57].
Performance monitoring includes the observation of the relationship between power, wind speed, rotor speed or blade angle. Large deviations may indicate a problem. Vibration analysis is the most known technology used for condition monitoring. In the low-frequency range position transducers can be used, and in the high-frequency common accelerometers are used. [25]
In order to enable vibration monitoring, vibrations of mechanical components to be mounted on wind turbines are standardized (see e.g. [29]). But vibration analysis condition monitoring compared with other condition monitoring technologies needs a special recording system needs, and a large amount of data (high sampling frequencies) needs to be recorded and treated. [37]
Table 2.1 states what the different condition monitoring methods can and cannot detect. Vibration and acoustic measurements at different locations at the drivetrain enable the estimation of the size and location of the crack. Acoustic emission measurements feature very high frequencies compared with other methods. The necessary high sampling rates lead to expensive data acquisition systems, which need to be considered when taking acoustic condition monitoring system should be installed [37]. Thermography directly indicates the position of the crack on the pictures. Oil monitoring enables, based on lubricant deterioration (measure of viscosity, water content, particle matter or degree of oxidation), finding indications that failure might soon occur. But the location of the crack cannot be indicated.
For the drivetrain components, acoustic and vibration analysis seem to be suitable [56] (Vibration measurements are very suitable for rotating devices). Challenges with vibration analyses and wind turbine applications are according to [25, 54] the dynamic load characteristics (not fixed rotational speed) and the low rotational speeds. An important aspect when implementing condition monitoring is the amount of data which needs to be analyzed in order to get tendencies for possible failures. Furthermore, the wind is a dynamic parameter which also introduces dynamics to the overall systems and makes it difficult to read out tendencies. It is, therefore, not enough to analyze each parameter isolated from the other. Another aspect to be aware of is that some wind turbine characteristics are (also within a wind turbine farm) different for each wind turbine.
Condition monitoring can only be used when the measured parameter is a reliable indicator of a certain failure

Table 2.1: Possibilities and limitations of different condition monitoring methods. [48]

CM method	Indication of		
	crack position in component	size of possible crack/damage	lubricant deterioration
Vibration analysis	X	X	
Acoustic measurement	X	X	
Oil monitoring		X	X
Thermography	X	X	
Performance	X	X	X

or prospective failure. Furthermore, knowledge about failure progress (time scale and how measured parameter changes) needs to be known. This indicates at which value of the measured parameter, replacement/repair as well as inspection need to be performed. Among the above mentioned different techniques, according to [48] and [57] vibration analysis, fibre optic strain gauges and oil monitoring (particle counters) are the most predominantly used condition monitoring techniques for wind turbine applications. Strain gauges mounted on rotating parts can be

used with slip rings or radio telemetry in order to transfer the measured results to the control unit. The reason for the application of vibration and oil quality analysis for condition monitoring are due to their cheap implementation, their proven and high availability (due to large experiences from other industry branches) as well as possibility for remote operation. Furthermore, these two condition monitoring technologies indicate different ranges of potential failures.
Furthermore, condition monitoring can be performed on-line or off-line. On-line monitoring enables deep insight in the performance analysis of the machine and shows characteristic changes over time. On-line can be applied for details which are not accessible or where (and this is the case for OWTs in general) access to the machine is generally costly and limited. Off-line monitoring means inspections at specific intervals by maintenance personnel.

2.1 What is used Today

There are tools available for (offshore) wind turbines in order to perform condition monitoring. The main focus for condition monitoring of OWTs is mainly on the rotor blades, the generator, the gearbox, the main bearings, the yaw and pitch system as well as the main bearings. There are different industrial tools available enabling on-line condition monitoring for drivetrain components of wind turbines. The bearing company SKF offers their condition monitoring tool called SKF WinCon [49], which also contains a remote lubrication system for monitoring the WT machines as well as lubrication system itself. For vibration analysis, existing tools used for other rotating components from PRÜFTECHNIK Dieter Busch AG (called VIBNODE® and VIBROWEB XP®) [44] can be used. Gram & Juhl A/S [24] offers their TCM® system which consists of accelerometers and sensors to perform online condition monitoring of wind turbines. Another company offering online condition monitoring tools is Brüel & Kjær Vibro GmbH [10] with their VibroSuite software package and their data acquisition unit. Mita-Teknik offers their MiCMS™ Condition Monitoring System [41] with real time frequency and time domain signal processing tools. Spectral analysis (including their spectral trends) and online monitoring of vibrations can be treated with FAG Industrial Services condition monitoring system WiPros [22].
Feedback from the condition monitoring should be used to improve existing and planned components. Therefore, the recorded data should be centralized stored in order to enable cross analysis and comparisons between sites and different turbine types as well as drive conclusions and improvements from a large number of monitored turbines. [10]

Chapter 3

Theoretical Background of Important Condition Monitoring Analysis Techniques

This section explains the theoretical background of the techniques used in this report for analysing condition monitoring investigations of a wind turbine main shaft.

3.1 Descriptive Statistics

A common way of describing statistics of a certain parameter is the use of the mean value μ and the standard deviation σ of a certain dataset $X = (x_1, x_2, ..., x_N)$ of one parameter for a recorded time-series with N recorded data points [5]:

$$\begin{aligned} \mu_X &= \frac{1}{N}\sum_{i=1}^{N} x_i \\ \sigma_X &= \sqrt{\frac{1}{N-1}\sum_{i=1}^{N}(x_i - \mu)^2} \end{aligned} \tag{3.1}$$

3.2 Fourier Transform

Fourier transforms enable the description of a measured/simulated sign $x(t)$ by means of a set of functions $e^{i\omega t}$:

$$x(t) = \frac{1}{2\pi}\int_{-\infty}^{\infty} X(\omega)e^{i\omega t}dt = \frac{1}{2\pi}\int_{-\infty}^{\infty} X(\omega)(\cos(\omega t) - i\sin(\omega t))dt \tag{3.2}$$

where ω represents the angular frequency and $X(\omega)$ the Fourier transform. Measured and simulated data is available at discrete data points. In such cases the Fourier transform can only be calculated at these discrete data points. Then, the so-called Discrete Fourier Transform (DFT) is applied. The DFT is defined for N data points as:

$$X_k = \sum_{n=0}^{N-1} x_n e^{\left(-i2\pi k \frac{n}{N}\right)} \tag{3.3}$$

where x_n are the Fourier coefficients (complex number) and can be calculated by the use of Fast Fourier Transforms (FFTs), which finds fourier coefficients for the different frequency bins.
The results from the FFT can be used to build the so-called Frequency Response Function (FRF) H, which is the ratio between an output of the system $Y(\omega)$ and a certain input of the system $X(\omega)$ for a given frequency ω:

$$H(\omega) = \frac{Y(\omega)}{X(\omega)} \tag{3.4}$$

3.3 Wavelet Transform Methods

A Wavelet transformation belongs to the family of time-frequency transformations. The advantage of Wavelet Transforms is their ability to get information about location and time, which is important for signals which vary in frequencies. The Wavelet theorem is based on the Heisenberg uncertainty principle [55], which states that high resolution in frequency and position cannot be obtained at the same time. When using Wavelet transforms, the frequency resolution of the time and position can be adapted. Wavelet transform methods are a tool capable of representing non-stationary processes.
Wavelet transforms can, in general, be categorized into two groups: continuous wavelet transforms (CWT) and discrete wavelet transforms (DWT). The CWT is based on a translational and scale change of the function $\Psi_{s,u}(t)$, which is also called mother wavelet and can be written as [40]:

$$\Psi_{s,u}(t) = \frac{1}{\sqrt{s}}\Psi\left(\frac{t-u}{s}\right) \tag{3.5}$$

where s is the scaling parameter and u the position parameter (also called translational factor). The basic wavelet $\Psi_{s,u}(t)$ has to fulfill the following basic properties:

$$\begin{aligned}\int_{-\infty}^{\infty} \Psi_{s,u}(t)dt = 0 \\ \int_{-\infty}^{\infty} \Psi_{s,u}^2(t)dt = 1\end{aligned} \tag{3.6}$$

The continuous wavelet transform $CWT_x(s,u)$ of a signal $x(t)$ is the decomposition of the signal $x(t)$ in a set of functions forming the base with the conjugate ($\Psi_{s,u}^*(t)$) of the wavelet $\Psi_{s,u}(t)$, (see e.g. [13]):

$$CWT_x(s,u) = \int x(t)\Psi_{s,u}^*(t)dt \tag{3.7}$$

However, continuous wavelet transforms contain redundant information and are computationally demanding. Therefore, so-called discrete wavelet transforms are often used for applications where computational time is limited (e.g. for online condition monitoring). Discrete wavelet transforms replace the continuous coefficients s and u in the CWT approach by sampling specific parameters. The DWT calculates the wavelet coefficients at discrete intervals (power of two intervals) of time and scale. The discrete wavelet transform, $DWT_x(j,k)$, is given as (see e.g. [16, 13]):

$$DWT_x(j,k) = \frac{1}{\sqrt{2^j}}\int x(t)\Psi^*\left(\frac{t-2^jk}{2^j}\right)dt \tag{3.8}$$

where j represents the discrete dilation and k the translation, respectively. The parameters j and k are integers. The transfer from CWT to DWT can be done by using the two equations:

$$\begin{aligned}s = 2^j \\ u = 2^jk\end{aligned} \tag{3.9}$$

The signals from the DWT result in low frequency approximation signals A (called approximation coefficients) and high frequency details D (called detail coefficients or wavelet coefficients). The original signal $x(t)$ can be reproduced by the signals A and D:

$$x(t) = A_j + \sum_{j\leq J} D_j \tag{3.10}$$

where J is the total number of considered levels. When using multilevel filtering ($j > 1$) repetition of the filtering process is applied. Figure 3.1 shows how multilevel filtering is performed for an example with three levels ($J = 3$). Wavelet transforms basically break the signal down into a series of local basis functions, which are called wavelets. The choice of the considered wavelet depends on the particular signal processing application and the requirements. There is no standard or general method for selecting the wavelet function for different tasks [43]. Several wavelet forms exist with unique properties and associated advantages and disadvantages. Among the most commonly used wavelet families in condition monitoring are the Daubechies, Biorthogonal, Symlet and Coiflet wavelets. Different studies as e.g. [34, 46] show that for rotating machinery the Daubechies mother wavelet family shows good results.
More general information about Wavelet transforms with respect to condition monitoring can be found e.g. in [43, 61].

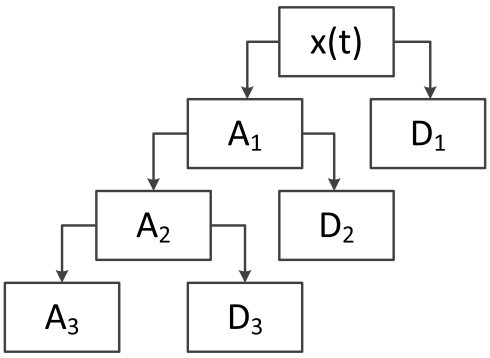

Figure 3.1: Example of Wavelet decomposition tree for multilevel filtering.

3.4 Modal Assurance Criteria

Modal assurance criteria (MACs) are a measure to compare the similarity of two mode shapes. MACs are statistical indicators sensitive to large differences and relatively insensitive to small differences in the mode shapes. MAC values have their origin in the comparison of analytical and experimental results (modal analysis and model updating). But this criterion can also be used in condition monitoring cases in order to detect possible damages (see e.g. [1]). A reduction in the modal assurance criterion value could indicate a damage of a structural detail. In the case of condition monitoring, the modal assurance criterion principle is used to compare the instantaneous characteristics (damaged stage) with the reference characteristics (undamaged stage). Changes in the modal assurance criterion values over time could indicate partly damaged components (e.g. crack evolution).
There are many different ways how a modal assurance criteria is defined and calculated. A good overview about the different methods is given in [3]. The two modal assurance criteria considered in this paper are explained in the following.
The Modal Scale Factor (MSF) is a mean number which normalizes the estimates of the same modal vector, taking into account magnitude and phase differences [3]. MSF represents the ratio between a certain discrete FRF (H) and a reference FRF (H_{ref}) [21]:

$$MSF = \frac{\sum_{\omega=\omega_1}^{\omega_2} H(\omega) \cdot H^*_{ref}(\omega)}{\sum_{\omega=\omega_1}^{\omega_2} H_{ref}(\omega) \cdot H^*_{ref}(\omega)} \tag{3.11}$$

where ω indicates the actual considered discrete frequencies within the considered frequency range between ω_1 and ω_2. For condition monitoring purposes, the reference FRF, H_{ref}, is the case when no crack/failure of the device is present. The second considered modal assurance criterion considered in this paper is the Frequency Response Assurance Criterion (FRAC), which estimates the linear consistency (degree of linearity) between two FRFs H and H_{ref} [3]:

$$FRAC = \frac{|\sum_{\omega=\omega_1}^{\omega_2} H(\omega) \cdot H^*_{ref}(\omega)|^2}{\sum_{\omega=\omega_1}^{\omega_2} H_{ref}(\omega) \cdot H^*_{ref}(\omega) \sum_{\omega=\omega_1}^{\omega_2} H(\omega) \cdot H^*(\omega)} \tag{3.12}$$

where H^* indicates the complex conjugated of the complex FRF vector H. FRAC values reach numbers between zero and unity. A value of 1 means a perfect match whereas a value of 0 means that the two shapes are completely dissimilar (no consistency). It needs to be mentioned that if the same errors (e.g. biases) are present in all FRF estimations, it cannot be detected by the FRAC and the MSF [3].
For condition monitoring purposes, the absolute value of MSF and FRAC is not of importance but its change over time (Comparison undamaged component and partly damaged components) is of importance. The MSF as well as the FRAC can be calculated over the overall frequency range or for a certain frequency range.

3.5 Time Synchronous Averaging

Time Synchronous Averaging (TSA) algorithms are commonly used for determining the condition of rotating equipment. TSA is a tool which enables the extraction of periodic waveforms from measured signals.
TSA averages numerous revolutions with a length corresponding to a single revolution. TSA enables the enhancement of the vibration frequencies which are multiples of the shaft frequency. TSA is widely used for condition monitoring of bearings or gearboxes because the TSA technique averages out random vibrations and external disturbances.

The results of the TSA can be performed either in the time domain or the frequency domain. Reference [8] compared different TSA techniques (spline, linear and bandwidth limited interpolation as well as frequency domain TSA). The results showed that the frequency domain TSA provided the best discrimination in the detection of faults.
Using TSA in the frequency domain based on a discrete Fourier transform (DFT), Equation 3.3 can be expanded by considering M rotations as well as N data points per rotation and can be written as [52]:

$$X_k = \sum_{n=0}^{N-1} \bar{x}_n e^{\left(-i2\pi k \frac{n}{N}\right)} = \sum_{n=0}^{N-1} \sum_{m=1}^{M} x_{n,m} e^{\left(-i2\pi k \frac{n}{N}\right)} \tag{3.13}$$

where $\bar{x}_n$ is the time-averaged data resulting from M data points and $x_{n,m}$ represents the nth Fourier coefficient of rotation number m.

Chapter 4

Condition Monitoring of Offshore Wind Turbine Main Shaft - Example

The lack of access to defect records and experience is according to [58] one of the main challenge to overcome when implementing condition monitoring systems. Also, in this example with focus on crack detection in the main shaft, no recorded data is directly available. Therefore, simulated data is considered.
The example considered in this study is based on simulations performed with FAST (Fatigue, Aerodynamics, Structures and Turbulence, v8.08) simulation tool, which is explained in more detail in [31]. The AeroDyn [15] v14.02.01 tool is used to determine the aerodynamic loads and the wind conditions based on the generalized dynamic wake model and the Blade-Element/Momentum theory, see [42]. The wind field used as input for the FAST simulations are generated by TurbSim (v1.06.00).
Table 4.1 shows the baseline definitions of the NREL 5MW offshore wind turbine. More background information about the considered wind turbine is given in [32]. The NREL 5MW baseline wind turbine contains a generator-torque controller which optimizes the power capture below the rated wind speed of 11.4 m/s as well as a blade-pitch controller which regulates the generator speed above the rated wind speed.
A PI pitch controller is considered for controlling the torque at the drivetrain. The torque defines, among others, the rotational speed of the main shaft as well as the electricity production. The generator is modeled as a variable-speed generator.
The generator is modeled using the Thevenin Equivalent Circuit equations for a three phase induction generator, and the considered gearbox has a gear transmission ratio of 97.
According to [11], are any condition monitoring decisions/guidelines based on numerical simulations and tests at

Table 4.1: General properties taken from [32] of the NREL 5MW Baseline Wind Turbine.

Meaning	**Value**
Rated Power	5 MW
Rotor Orientation, Configuration	Upwind, 3 Blades
Control	Variable Speed, Collective Pitch
Drivetrain	High Speed, Multiple-Stage Gearbox
Rotor, Hub Diameter	126 m, 3 m
Hub Height	90 m
Cut-In, Rated, Cut-Out Wind Speed	3 m/s, 11.4 m/s, 25 m/s
Cut-In, Rated Rotor Speed	6.9 rpm, 12.1 rpm
Rated Tip Speed	80 m/s
Overhang, Shaft Tilt, Precone	5 m, 5^o, 2.5^o
Rotor Mass	110,000 kg
Nacelle Mass	240,000 kg
Tower Mass	347,460 kg

laboratory scale. The issue of whether or not environmental effects can be reliably and confidently filtered from measured data for condition monitoring purposes has not yet been tackled comprehensively in the literature.

4.1 Stochastic Model

In order to make the results realistic and stochastic, uncertainties of different input parameters are considered and the results are based on Monte Carlo simulations.
The following environmental input parameters are considered as stochastic variables:

- Turbulence intensity and mean wind speed within bin.
- Significant wave height and wave peak period given a certain wind speed (location dependent).

The turbulence intensity of the actually considered 10-minute wind speed within a given 10-minute mean wind speed bin are considered as stochastic variable. Its mean value is set equal to 0.15 at hub height and its uncertainty has a Coefficient of Variation value ($COV = \sigma/\mu$) equal to 0.05 [50]. Furthermore, the 10-minute mean wind speed at hub height itself is modeled as uniformly distributed for a given wind speed bin with width b (commonly 1 m/s). Table 4.2 shows the considered stochastic model. Time series with a length of 10-minutes are performed as considered in other studies (see e.g. [58]).
The turbulence dependent on the height is assumed to follow the so-called normal turbulence model (NTM) and the mean wind speed dependent on the height follows the power law with an exponent of 0.14 as proposed by [27] for normal conditions. The Kaimal spectral density model, which is in accordance with the standards [26] and [17] for offshore applications, is considered for modeling the wind energy distribution among different frequencies. The waves are assumed to follow a Pierson/Moskowitz spectrum.
Wind loads as well as hydrodynamic loads due to waves are considered in the simulations. For wind turbine applications, the wave states can be modeled conditional on the wind speed. The waves are characterized with the significant wave height and the peak period. Reference [12] presents, based on measurements at HornsRev in the Danish North Sea, a model for the significant wave height conditional on the mean wind speed V. The peak period can, according to [18], be assumed to follow a Lognormal distribution conditional on the significant wave height. The peak period stochastic variables are taken following the North Sea region characteristics (Nautic zone 11 in [18], Appendix B and C).

Table 4.2: Environmental parameter for the different FAST simulations with a duration of 10 minutes. U: uniform distribution; N: Normal distribution; LN: Lognormal distribution; D: deterministic; b: bin size (here 1 m/s); Distr.: distribution; Std.: standard.

Meaning	**Distr. type**	**Mean value**	**Std. deviation**	**Source**
10-minute wind speed V	U	V_m	$\left[\frac{(b+1)^2-1}{12}\right]^{0.5}$	
Turbulence intensity k	N	0.15	0.0075	[50]
Significant wave height H_S for given V_m	N	$0.13 \cdot V_m$	0.24 m	[12]
Peak period T_P given certain $H_S = h$	LN	$\sqrt{2}\exp\left[0.7 + 0.935 \cdot h^{0.222}\right]$	$\sqrt{2}\exp\left[0.07 + 0.1386\exp(-0.222 \cdot h)\right]$	[18]
Water depth	D	20 m	-	-

4.2 Crack Modeling

The idea of this study is to investigate which condition monitoring technique is suitable to detect cracks in the main shaft as well as which parameter/measurements are needed in order to be able to detect cracks in the main shaft of a wind turbine using condition monitoring. The following parameters are investigated in this study for possible main shaft crack indicator:

- Power production
- Pitch angle adjustment
- Rotational speed shaft
- Acceleration of shaft speed

- Torque shaft behavior

Reference [1] uses capacitive acceleration measurements on the blades for detecting damage in the blades. Wind turbine main shafts have large torsional loads and are exposed to complex transient torsional loading, which may initiate cracks and let initiated cracks or manufacturing defects propagate. In this example, open cracks on the surface are considered. Cracks on the surface of the main shaft can e.g. be initiated during the production process itself or by circumferential scratches on the shaft surface due to sliding between the main shaft and the planetary frame [59]. These surface cracks are then exposed to cyclic loading which increases the crack size over time and will lead after a certain time to fatigue failure.
The drivetrain is modeled in the FAST tool as an equivalent shaft separating the hub and the generator. This shaft is modeled as a shaft with a linear torsional stiffness and as isotropic linear elastic material. Based on simulations and experiments on rotating shafts, reference [7] detected that the torsional stiffness decreases when cracks are present. Furthermore, [7] noted that the reduction of torsional stiffness is generally higher than the reduction of bending stiffness for cracks. In this study it is assumed that when cracks in the main shaft (low speed shaft) occur, the torsional stiffness is affected. Reference [35] investigated the effect of semi-elliptical surface cracks on torsional stiffness by experiments and FEM studies. The torsional stiffness $k_{undamaged}$ of an undamaged shaft can be calculated for isotropic materials as:

$$k_{undamaged} = \frac{GJ}{L} \tag{4.1}$$

where J is the torsion constant, G the shear modulus and L the length of the element. For cracked shafts the resulting torsional stiffness, $k_{damaged}$, can be calculated from the undamaged torsional stiffness $k_{undamaged}$ [35]:

$$k_{damaged} = k_{undamaged}\frac{\kappa}{1-\kappa} \tag{4.2}$$

where κ is the effective torsional stiffness and dependent on the crack size and form. Table 4.3 presents the κ values dependent on the crack size a and shaft diameter D value. Large a/D ratios are critical as large cracks have a large crack growth rate which can lead to residual failure of the main shaft after a short period. This study does not investigate the time-dependent crack growth of cracks but the short-time behavior (without considering crack growth) of a wind turbine given a certain crack size on the wind turbine shaft. The undamaged torsional stiffness $k_{undamaged}$ of the main shaft is equal to $8.68E+08$ Nm/rad [32].
For calculating the torsional stiffness value the model in Equation 4.2 is used and this model is connected to

Table 4.3: Effective torsional stiffness coefficient κ for different a/D ratios. Data is taken from [35].

crack depth a and Diameter D ratio (a/D)	**Effective torsional stiffness coefficient κ (-)**
0.1	1.44E-01
0.2	3.25E-02
0.3	8.33E-03
0.4	3.35E-03

uncertainties (model uncertainties). In order to account for these uncertainties, the torsional stiffness $k_{damaged}$ is combined with a stochastic variable X_k, which accounts for model uncertainties related with the torsional stiffness given a certain crack size a:

$$k_{model} = k_{damaged} \cdot X_k \tag{4.3}$$

where k_{model} is the torsional stiffness implemented in the FAST simulation. Reference [33] suggests to use a LogNormal distribution for the stochastic variable X_k with a mean value of 1 and a standard deviation of 0.1 for model uncertainties related with shear loads.
In general, the operators prefer keeping the condition monitoring analysis process as simple as possible, and the process should be based on already recorded parameters (e.g. for the control system). Complex condition monitoring systems may be expensive (additional costs). Not considered in this paper is the impact of failure of a certain component other than the main shaft (like e.g. imbalance of the blades or wear failure of the bearings) on the considered condition signals. This paper considers ideal conditions (no failure of other components). Common vibration condition monitoring setups have a recording frequency between 200 and 500 Hz. For the FAST simulation tool, a sample frequency of 200 Hz is chosen.

Chapter 5

Results

The purpose of this paper is not defining failure of the main shaft, but showing the relations between performance and the crack size (condition) of the main shaft. The results can e.g. be used to define threshold values when an inspection should be performed.
This example focuses on main shaft condition monitoring separated from other components. What is not answered in this example is the fact that crack growth of different components may occur at the same time and then interaction between e.g. the main shaft and the bearing impact the recorded data. But when the bearing is also condition monitored, these condition monitoring devices indicate imbalance and then inspection needs to be performed.
For each wind speed condition between 3 m/s and 25 m/s 50 10-minute simulations are performed within a certain 1 m/s bin in order to get statistical meaningful results for different a/D ratios and used as basis for the condition monitoring analysis. The results are discussed with the wind speed as a reference.

5.1 Time Domain Analysis - Simple Descriptive Statistics

The simulation results in this section are analyzed based on descriptive statistics. The results of the analyzed parameters (power production, pitch movement, torque measurements and rotational speed as well as rotational accelerations of the low speed shaft) are shown in Figure 5.1 dependent on the 10-minute wind speed for different crack depth a and main shaft diameter D ratios. In order to get an overview about possible main shaft crack indication parameters, Figure 5.1 shows the undamaged (a/D=0.0) and a damaged case (a/D=0.2). Mean values and the standard deviation of the considered parameters are shown including their standard deviations. Also, the skewness and kurtosis of the considered parameters in Figure 5.1 are analyzed but not shown here because they cannot be used as main shaft crack indicator. The results in Figure 5.1 show that below the rated wind speed (rated wind speed in this case at 11.4 m/s [32]) the uncertainties and variations among the different simulations are larger compared with wind speeds above the rated wind speed. Therefore, when using descriptive statistics cracks can only be detected at wind speeds above the rated wind speed. Figure 5.1 shows that only the standard deviation of the Low Speed Shaft (LSS) rotational acceleration has large enough differences between the two considered cases and thus makes it possible to identify a possible crack in the main shaft. All other parameters do not show differences large enough to identify possible cracks in the main shaft.
The only parameter which is able to clearly indicate cracks in the main shaft is shown in Figure 5.2 for further a/D ratios. Figure 5.2 shows the standard deviation behavior of the LSS acceleration based on 10-minutes of wind speeds simulations for a/D ratios between 0.1 and 0.4 together with the results from the undamaged main shaft (a/D=0.0). In general, it can be seen that for 10 minute mean wind speeds below the rated wind speed, the fluctuations of the accelerations are too large for all considered a/D ratios. But when having larger wind speeds than the rated wind speed, the standard deviation of the LSS acceleration becomes less scattered for all considered a/D ratios. However, a clear and explicit detection based on the LSS accelerations can only be performed when the crack is already relatively large. For a/D ratios above 0.2, the differences between the damaged and undamaged case become large enough such that the larger standard deviation of the acceleration explicitly indicates the crack in the main shaft of the drive train.
Figure 5.2 shows that, compared with the less damaged main shaft cases a heavily damaged main shaft (a/D=0.4) leads to different main shaft acceleration characteristics where large variations in LSS accelerations are also present at wind speeds between 8 and 15 m/s. This fact suggests that at this damage level other performance parameters can also indicate the damages in the main shaft.
Figure 5.3 shows the behavior of the power, the LSS torque and the LSS rotational speed for a damage level equal to a/D=0.4. The power curve indicated by the mean extracted power dependent on the wind speed is clearly

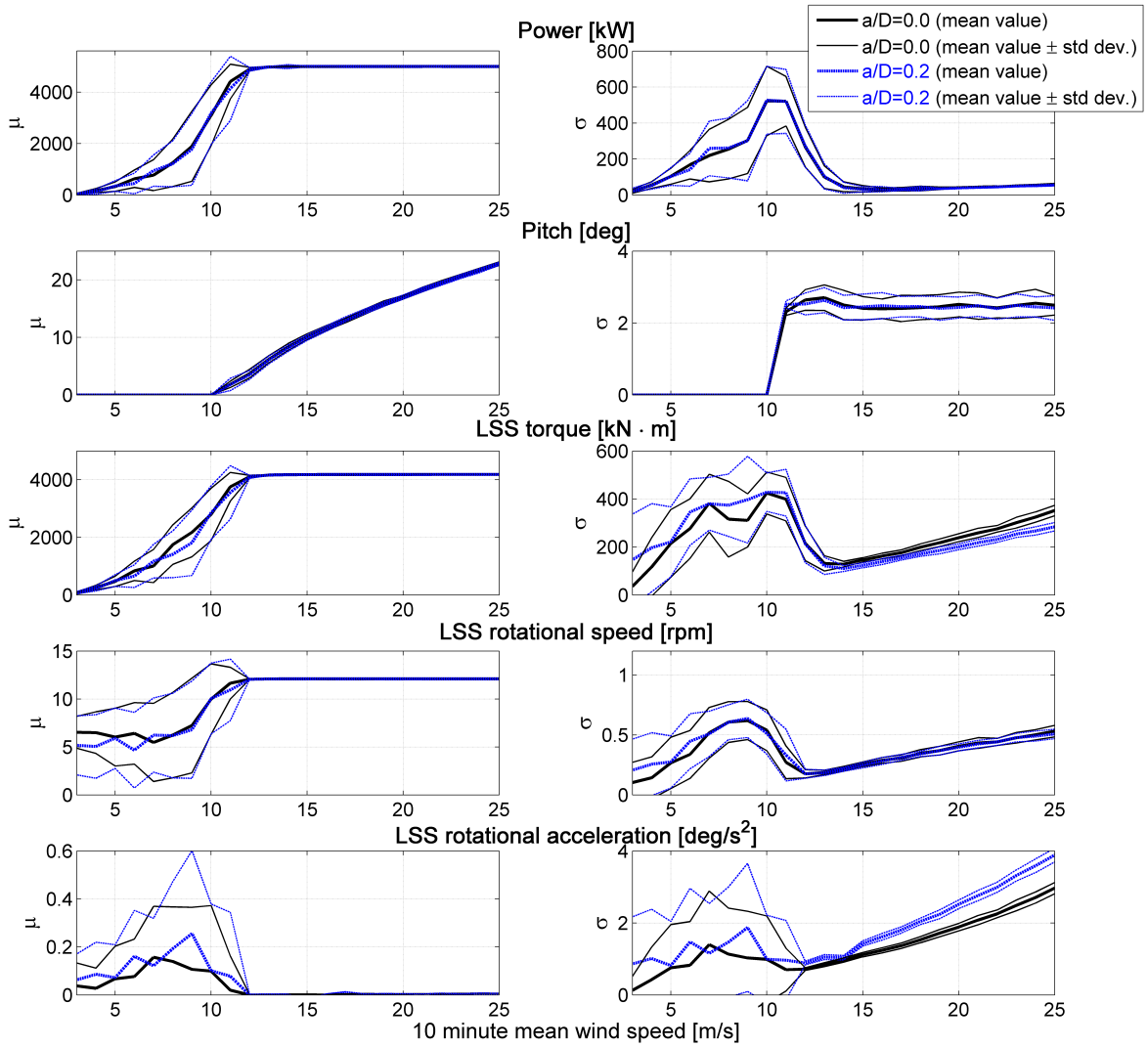

Figure 5.1: Mean value μ and standard deviation σ (including their standard deviations) of different performance parameters for different crack depth a and main shaft diameter D ratios dependent on 10-minute mean wind speeds between 3 m/s and 25 m/s. a/D=0.0: undamaged case; a/D=0.2: damaged case; LSS: low speed shaft.

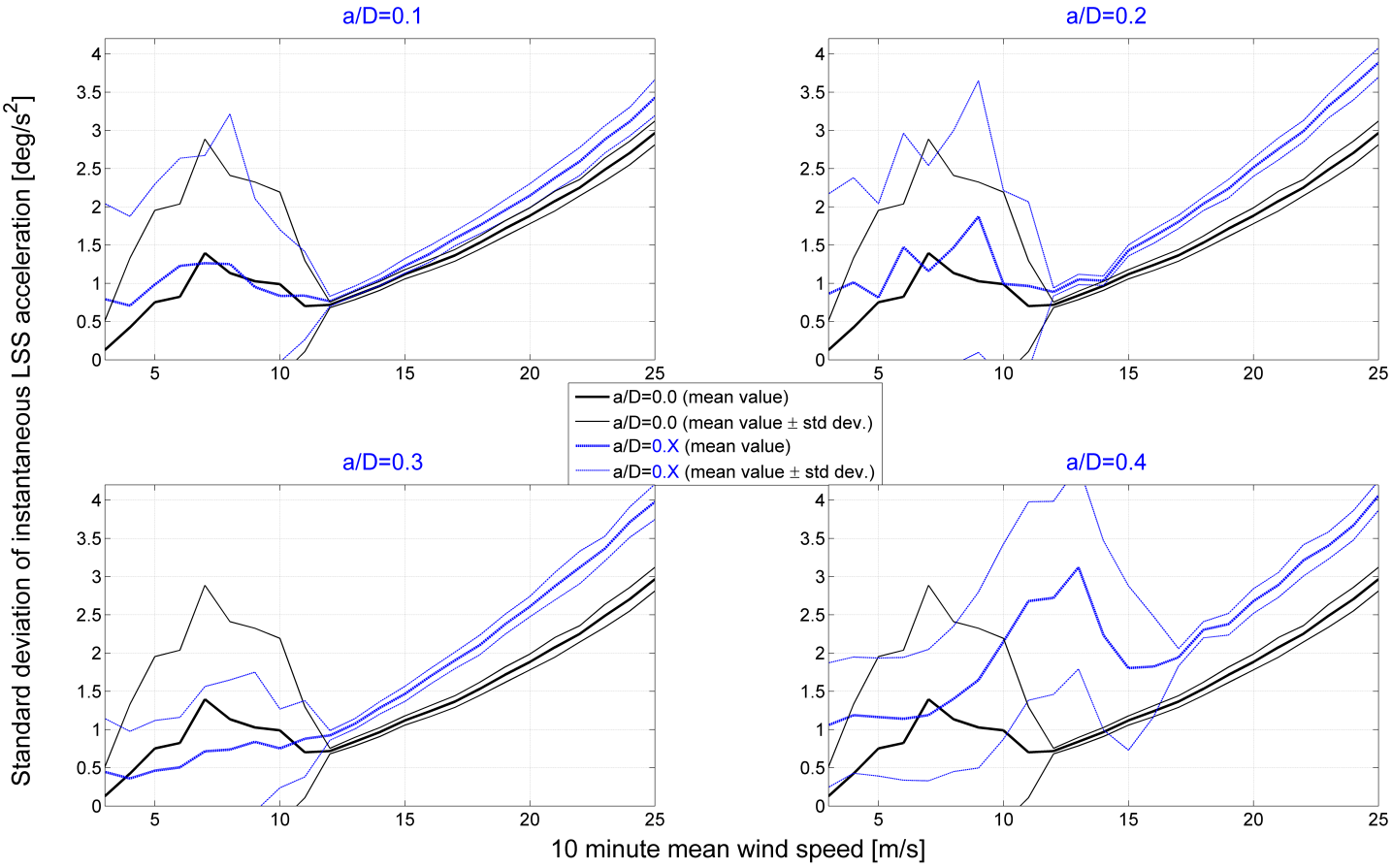

Figure 5.2: Standard deviation (its mean value and the corresponding standard deviation) of the instantaneous LSS acceleration for different crack depth a and main shaft diameter D ratio dependent on 10-minute mean wind speeds between 3 m/s and 25 m/s. LSS: low speed shaft.

decreased for 10-minute mean wind speeds between 8 m/s and 16 m/s. Also, the torque and the rotational speed of the LSS is smaller for mean wind speeds between 8 m/s and 15 m/s compared with the undamaged case. The aforementioned three parameters can also be used as damage indicators of the LSS main shaft for damage levels equal to a/D=0.4 or higher.

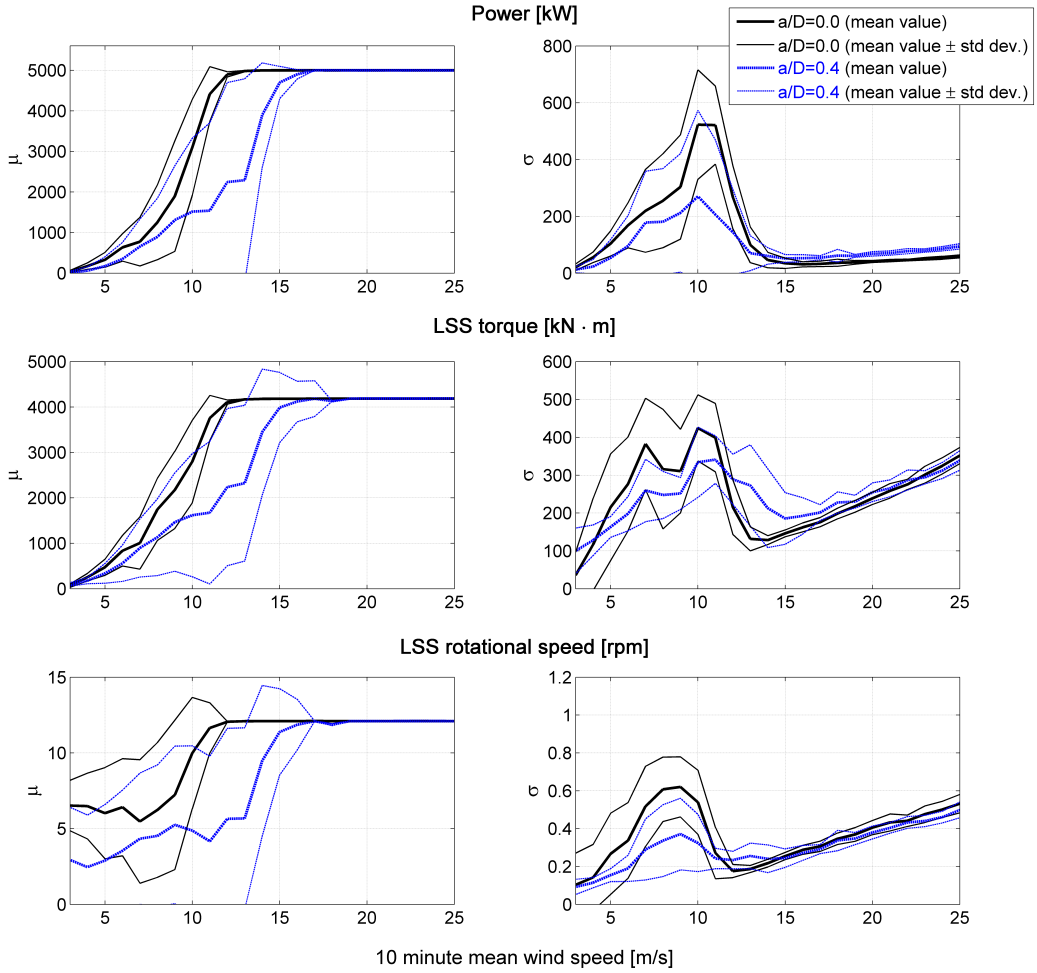

Figure 5.3: Mean value μ and standard deviation σ (including their standard deviations) of different performance parameters for different crack depth a and main shaft diameter D ratios dependent on 10-minute mean wind speeds between 3 m/s and 25 m/s. a/D=0.0: undamaged case; a/D=0.4: heavily damaged case; LSS: low speed shaft.

5.2 Frequency Domain Analysis - Simple Fast Fourier Transformation

The analysis of the frequency domain results given different main shaft crack depths can, among others, be performed by analyzing the frequency at which the spectral density value is maximized or the variation of the spectral density by investigating the spectral density for different crack depths over a certain frequency range.
Figure 5.4 shows the frequencies at which the spectral density values of the low speed shaft rotational acceleration are maximized for three different frequency ranges and different crack sizes at the main shaft. For a frequency range between 1 Hz - 2.8 Hz and 2.8 Hz - 5 Hz, the frequency of maximum spectral density values of the LSS acceleration is different for the two considered crack sizes, which enables detection of cracks on the main shaft. The lowest considered frequency range in Figure 5.4 (Frequency range 0.3 Hz - 1 Hz) does not show differences in the resulting frequencies where the spectral density is maximized for different crack sizes. Figure 5.4 shows that the large differences of the frequency at the maximum spectral density value of the rotational acceleration of the LSS within the frequency range of 2.8 Hz - 5 Hz is a useable parameter to indicate possible cracks in the main shaft. This frequency range (2.8 Hz - 5 Hz) enables indication the main shaft cracks at all 10-minute mean wind speeds in which the turbine is operating.

Figure 5.5 shows the expected frequency where the low speed shaft rotational acceleration spectral density value is

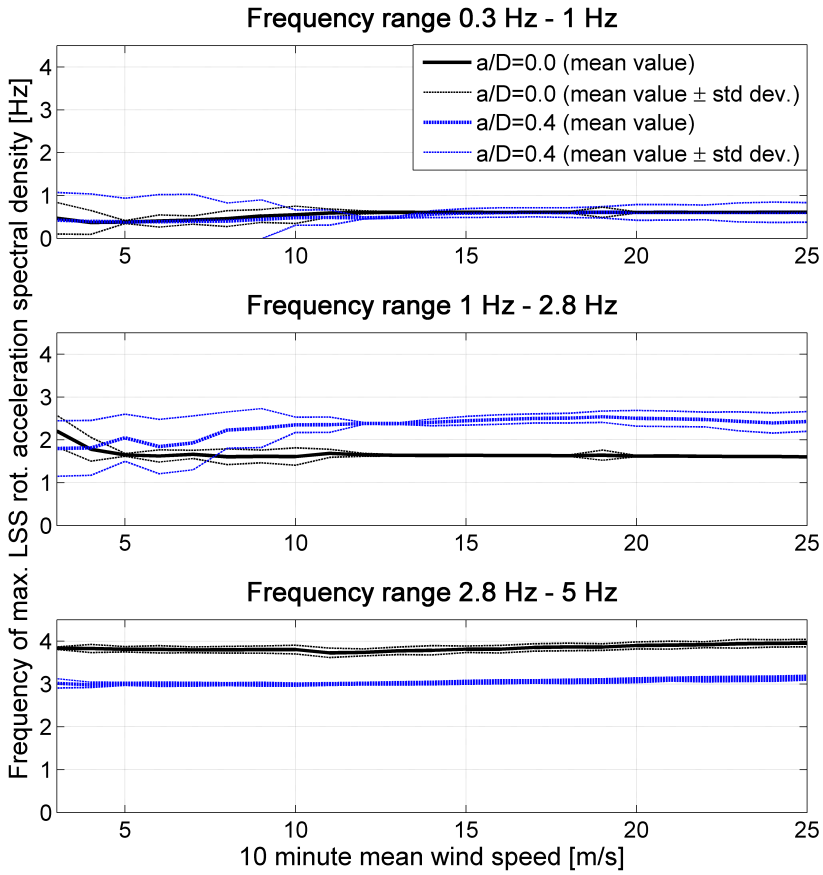

Figure 5.4: Frequency where low speed shaft (LSS) rotational acceleration spectral density values are maximized for different crack depth a and main shaft diameter D ratio dependent on 10-minute mean wind speeds between 3 m/s and 25 m/s for three different frequency ranges. a/D=0.0: undamaged case; a/D=0.4: heavily damaged case; max.: maximum; rot.: rotational.

maximized for different crack depth a and main shaft diameter D ratio dependent on 10-minute mean wind speeds between 3 m/s and 25 m/s for the frequency range 2.8 Hz - 5 Hz. The frequency at which the maximum rotational acceleration density values are reached decreases if the crack size increases. Figure 5.5 shows that a crack with a a/D ratio equal to 0.1 can be detected except for 10-minute mean wind speeds around the rated wind speed (10-15 m/s) where the difference to the undamaged case is not large enough. It needs to be kept in mind that under real conditions the accuracy of the measurement device and the risk of false alarms might as well influence the threshold for clear crack detection. A clear crack detection for all 10-minute mean wind speeds which the turbine is under operation is possible when the crack depth is equal to or larger than 20% of the main shaft diameter.
Instead of focusing on the maximum spectral densities within a certain frequency range, the spectral density distributions within a frequency range can be investigated. For this case study, investigations showed that the interesting frequencies are between 1 Hz and 5 Hz. Figure 5.6 shows the spectral density of the low speed shaft for different crack sizes having a 10-minute mean wind speed of 15 m/s. Depending on where the threshold for an alarm is set, indication of a crack might be possible already at a a/D ratio of 0.1 (comparison of the spectral density around 2.5 Hz). Perhaps the differences are too low such that many wrong alarms (alarms without real damage as the threshold is too low). But a a/D ratio of 0.2 shows clear differences in spectral density characteristics of the LSS rotational acceleration for frequencies between 1 Hz and 5 Hz compared with the undamaged case. Another factor indicating cracks in the main shaft is the frequency shifts of the spectral density peaks, which are already indicated by Figures 5.4 and 5.5.
Figure 5.6 shows the mean value and the standard deviation of the spectral density for a frequency range between 1 and 5 Hz for different crack depth a and main shaft diameter D ratios for a 10-minute mean wind speed of 15

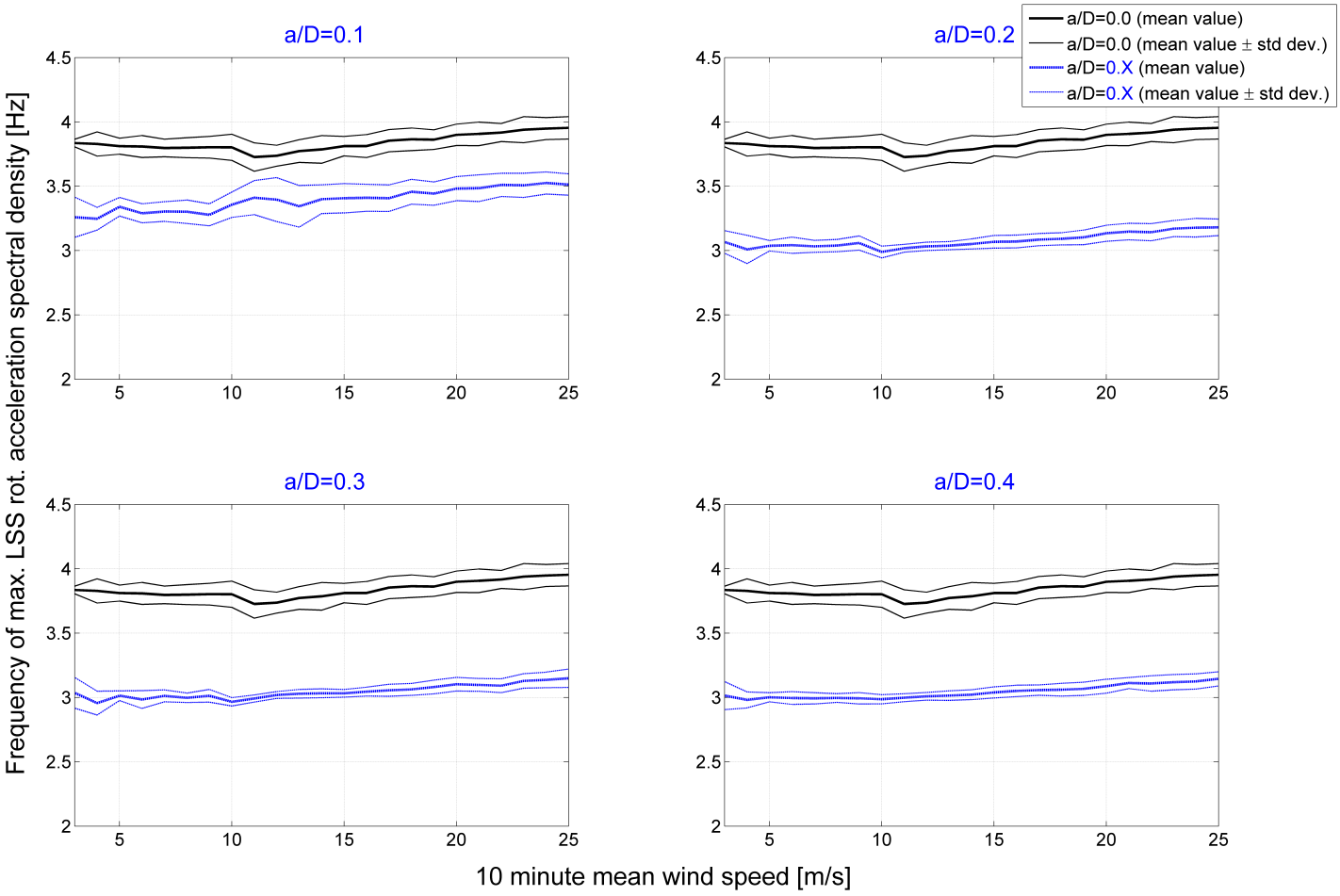

Figure 5.5: Frequency at which the LSS rotational acceleration spectral density is maximized for different crack depth a and main shaft diameter D ratio dependent on 10 minute mean wind speeds between 3 m/s and 25 m/s for a frequency range of 2.8 Hz to 5 Hz. max.: maximum; rot.: rotational.

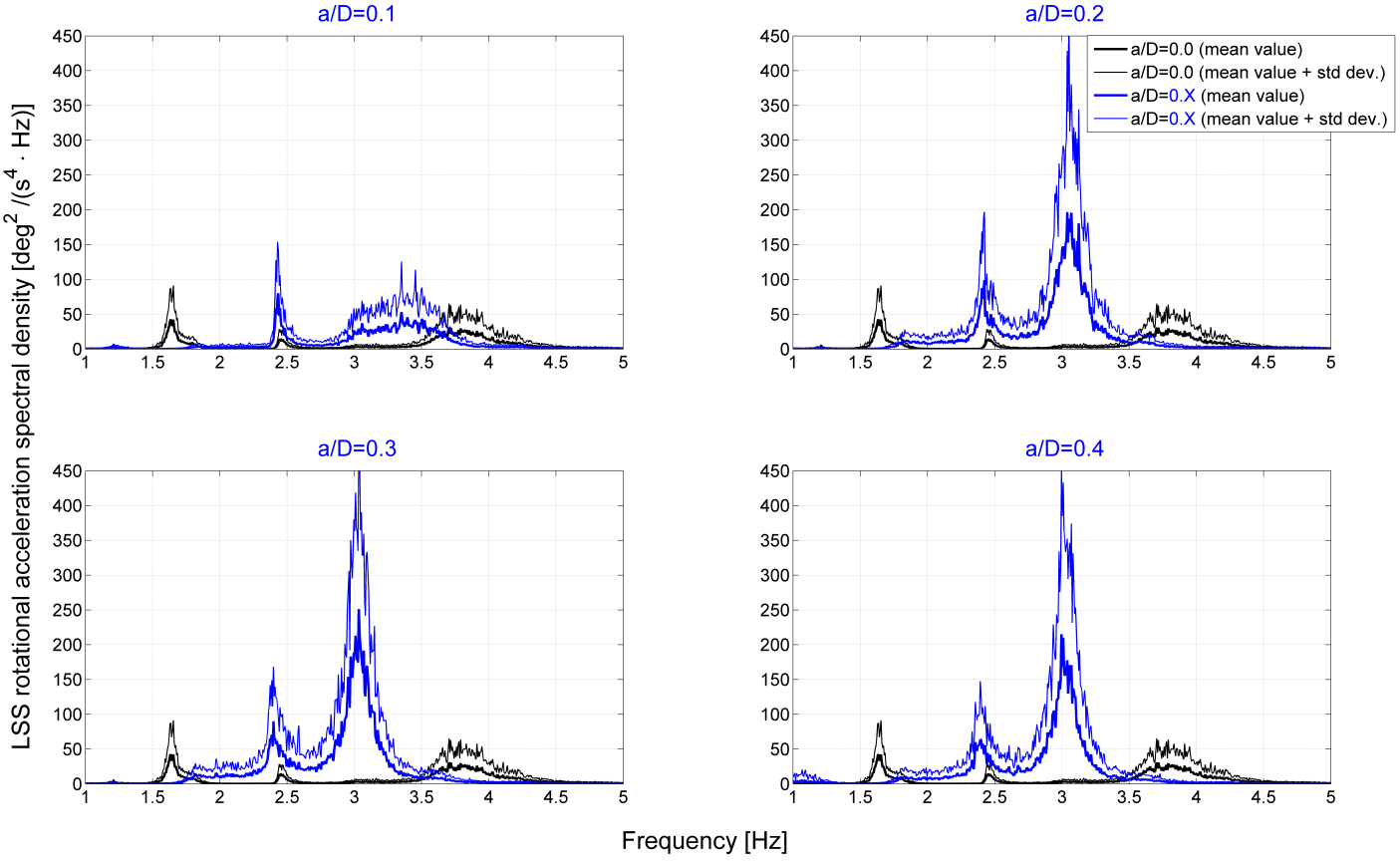

Figure 5.6: Spectral density of the LSS rotational acceleration for different crack depth a and main shaft diameter D ratio for a 10-minute mean wind speed of 15 m/s. std dev.: standard deviation; rot.: rotational; acc.: acceleration.

m/s. This figure shows that a 10-minute mean wind speed of 15 m/s is possible when the crack size to main shaft diameter ratio is equal to or larger than 0.2. Figure 5.7 shows the spectral density of the LSS rotational acceleration for different 10-minute mean wind speeds. The behavior between no main shaft crack and the case in which the a/D ratio is equal to 0.2 is considered in Figure 5.7. The amplitudes of the spectral density increase if the 10-minute mean wind speed is increased. This means that the condition monitoring alarm threshold should be dependent on the actual wind speed. But the frequencies at which the maximum spectral density of the rotational LSS acceleration occurs is, as shown in Figures 5.4 and 5.5, not dependent on the 10-minute mean wind speed.

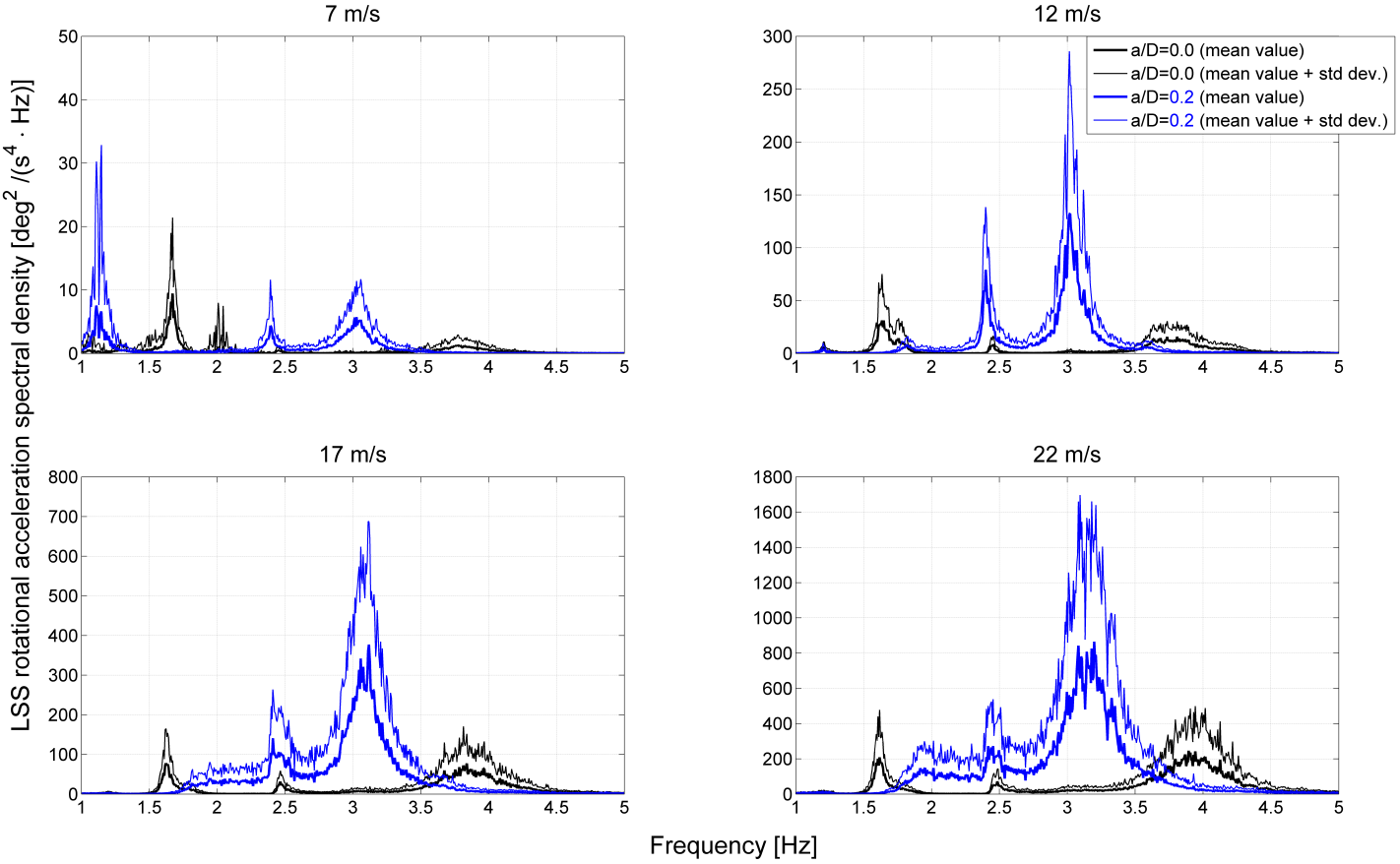

Figure 5.7: Spectral density of the LSS rotational acceleration for different 10-minute wind speeds at a crack depth a and main shaft diameter D ratios of 0.0 and 0.2. std dev.: standard deviation; rot.: rotational; acc.: acceleration.

5.3 Frequency Domain Analysis - Modal Assurance Criteria

Figure 5.8 shows the Modal Scale Factor (MSF) which is the ratio between the frequency response of a damaged main shaft with a a/D ratio between 0.1 and 0.3 and the frequency response of the undamaged case (a/D=0.0). This Figure shows the MSF when considering the frequency ranges between 2 Hz and 5 Hz as well as between 5 Hz and 10 Hz. The MSF becomes smaller when the damage is increased. But the differences in the MSF for different crack sizes at the main shaft are too small in order to explicitly detect the crack.
A better factor for indicating cracks on the main shaft is the Frequency Response Assurance Criterion (FRAC), which estimates the linear consistency between two Frequency Response Functions (FRFs). As a reference FRF, the undamaged case is considered. Figure 5.9 shows the FRAC for different crack sizes (a/D ratios between 0.1 and 0.3) dependent on the 10-minute mean wind speed and two frequency ranges (2-5 Hz and 5-10 Hz). Considering the frequency range between 2 Hz and 5 Hz by looking at the FRAC values, it indicates crack sizes for all considered 10-minute mean wind speeds whereas the frequency range between 5 Hz and 10 Hz leads to too small FRAC differences between different damage levels. Furthermore, the larger the crack size a is, the lower is the FRAC value.

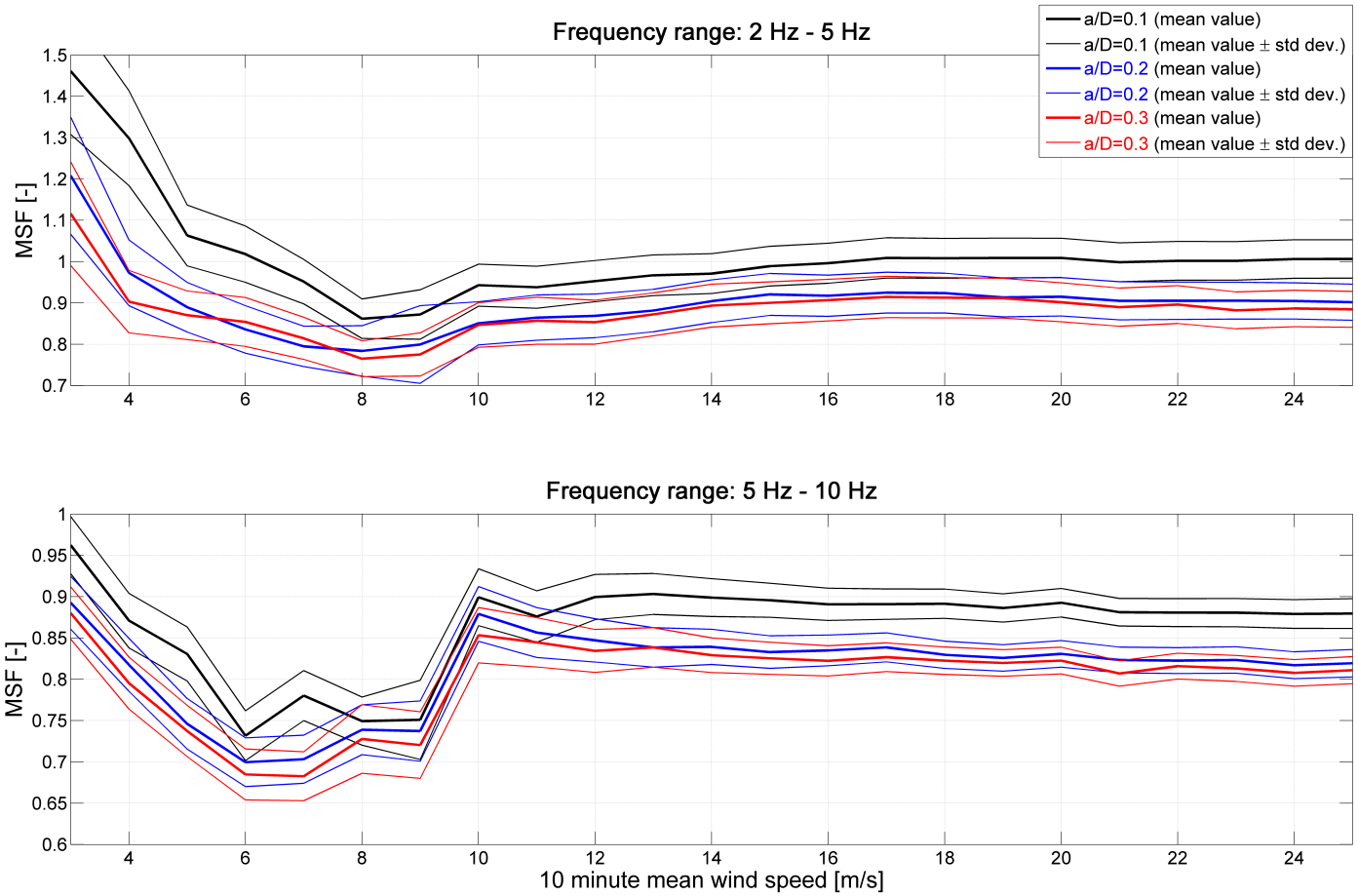

Figure 5.8: Modal Scale Factor (MSF) of the LSS rotational acceleration for different 10-minute wind speeds at crack depth a and main shaft diameter D ratios between 0.1 and 0.3. std dev.: standard deviation.

In this example, the FRAC (see Figure 5.9) is better suitable than the MSF (see Figure 5.8) for detecting cracks in

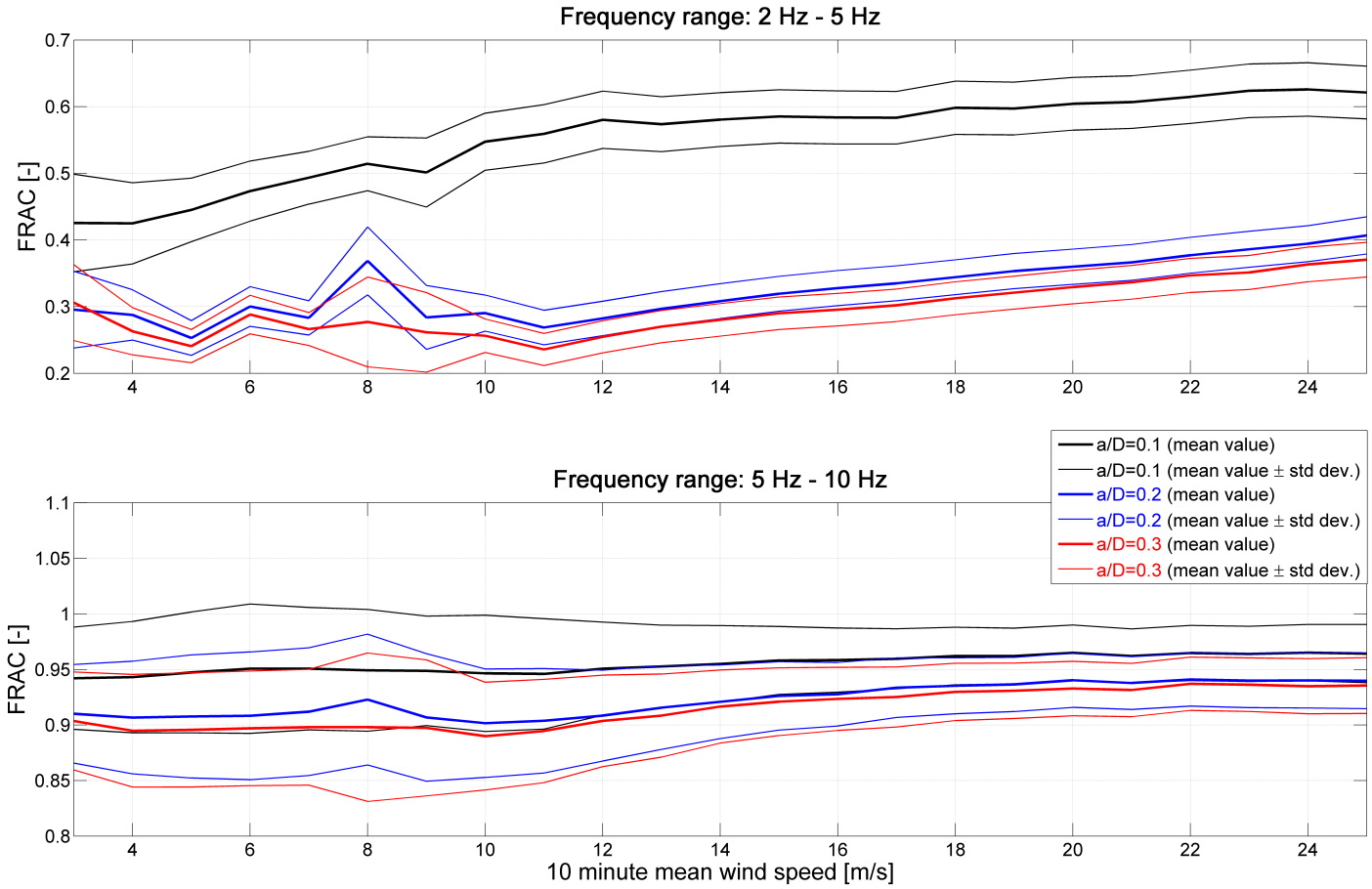

Figure 5.9: Frequency Response Assurance Criterion (FRAC) of the LSS rotational acceleration for different 10-minute wind speeds at crack depth a and main shaft diameter D ratios between 0.1 and 0.3. std dev.: standard deviation.

the main shaft.

5.4 Frequency Domain Analysis - Wavelet Transformation

In this section, Wavelet transformation based on a one-dimensional Wavelet decomposition is performed for the rotational acceleration of the LSS. Wavelet coefficients from discrete Wavelet transform (DWT) for 5 different levels (1-5) are considered. Table 5.1 shows which frequency range is covered by which level. The different levels make it possible to investigate different frequency ranges. This example will include Wavelets of the Daubechies type.
Figure 5.10 shows the mean value and standard deviation of the Wavelet coefficients D_j of the rotational LSS

Table 5.1: Corresponding frequency range of the different levels of the discrete Wavelet transform.

Level j	**Frequency range [Hz]**
1	0 - 100
2	0 - 50
3	0 - 25
4	0 - 12.5
5	0 - 6.25

rotational acceleration for different levels j. The undamaged case with no cracks present on the main shaft (a/D

ratio equal to 0.0) and the damaged cases with a a/D ratio equal to 0.2 are compared in Figure 5.10. This figure shows that the variation of the wavelet coefficients at the levels 1 and 5 indicates the crack with a crack depth a and main shaft diameter D ratio of 0.2. All mean values of wavelet coefficients at these 5 levels as well as the standard deviations of the wavelet coefficients at level 2, 3 and 4 do not indicate different values with and without the presence of a crack.
Figure 5.11 shows the variation of the wavelet coefficients of levels 1 and 5 dependent on the ratio a/D. Based

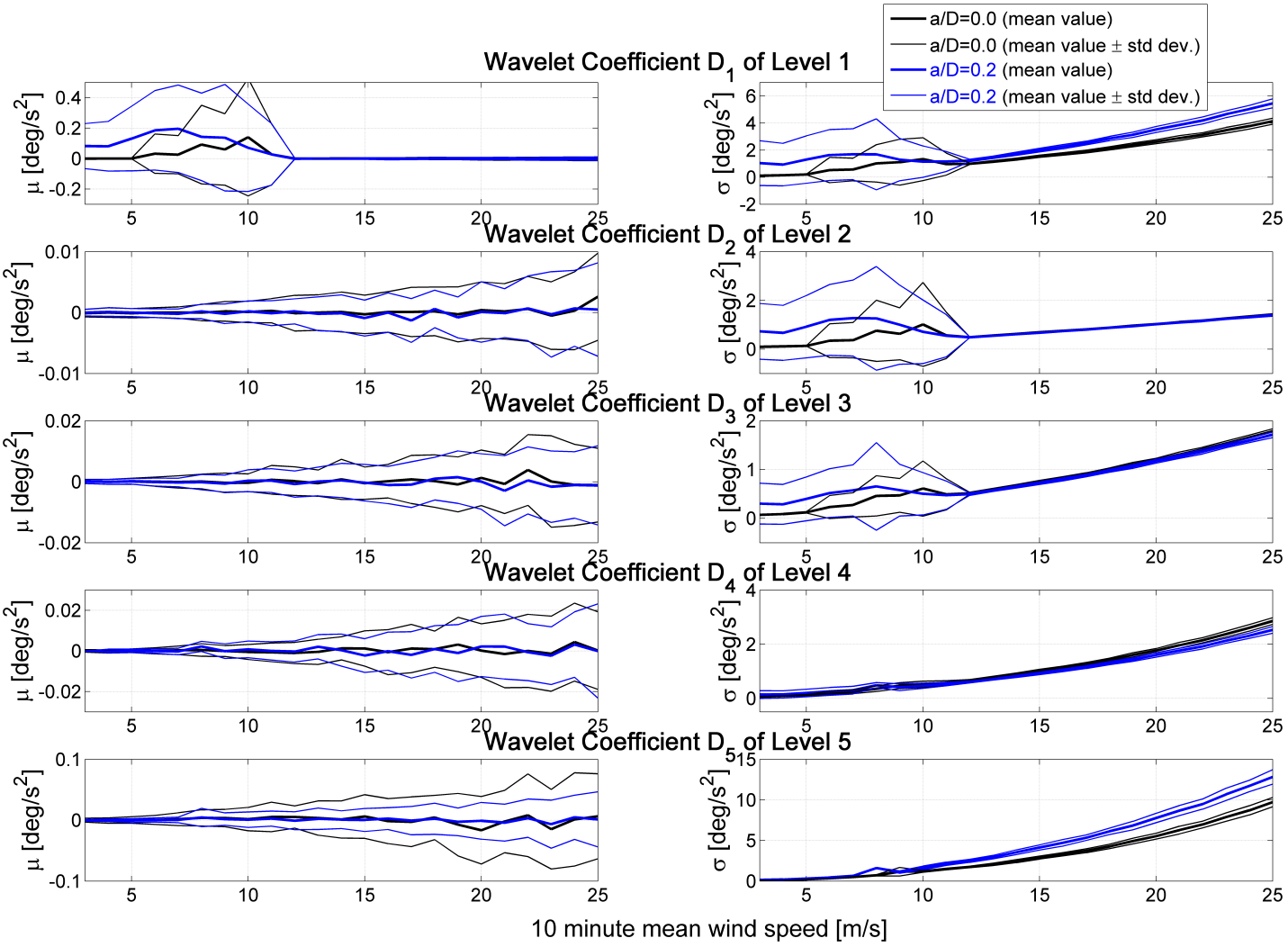

Figure 5.10: Mean value μ and standard deviation σ of the wavelet coefficients of the LSS acceleration time series considering 5 different levels, different 10 minute mean wind speeds and two different crack depth a and main shaft diameter D ratios of 0.0 and 0.2.std dev.: standard deviation.

on this figure one can estimate the minimal crack size, which enables detection of the crack when using Wavelet transformation in condition monitoring of the LSS. A crack size a to main shaft diameter D ratio of 0.1 does not give enough large different wavelet coefficient fluctuations at levels 1 and 5 to detect the crack. In general, the distinction between damaged main shaft case and the case in which no damage is present becomes bigger the larger the wind speed becomes. The differences in wavelet coefficient variations between a/D=0.2 and a/D=0.3 are small. It can be concluded that a minimal crack size equal to 20 $\%$ of the diameter can be detected when monitoring the LSS acceleration and performing wavelet transformations for 10-minute wind speeds larger than the rated wind speed.

5.5 Frequency Domain Analysis - Time Synchronous Averaging

An adapted Matlab®routine for TSA in the frequency domain using linear interpolation presented in [52] was used in this example. Before analyzing the TSA results, a sensitivity analysis on the number of considered rotations

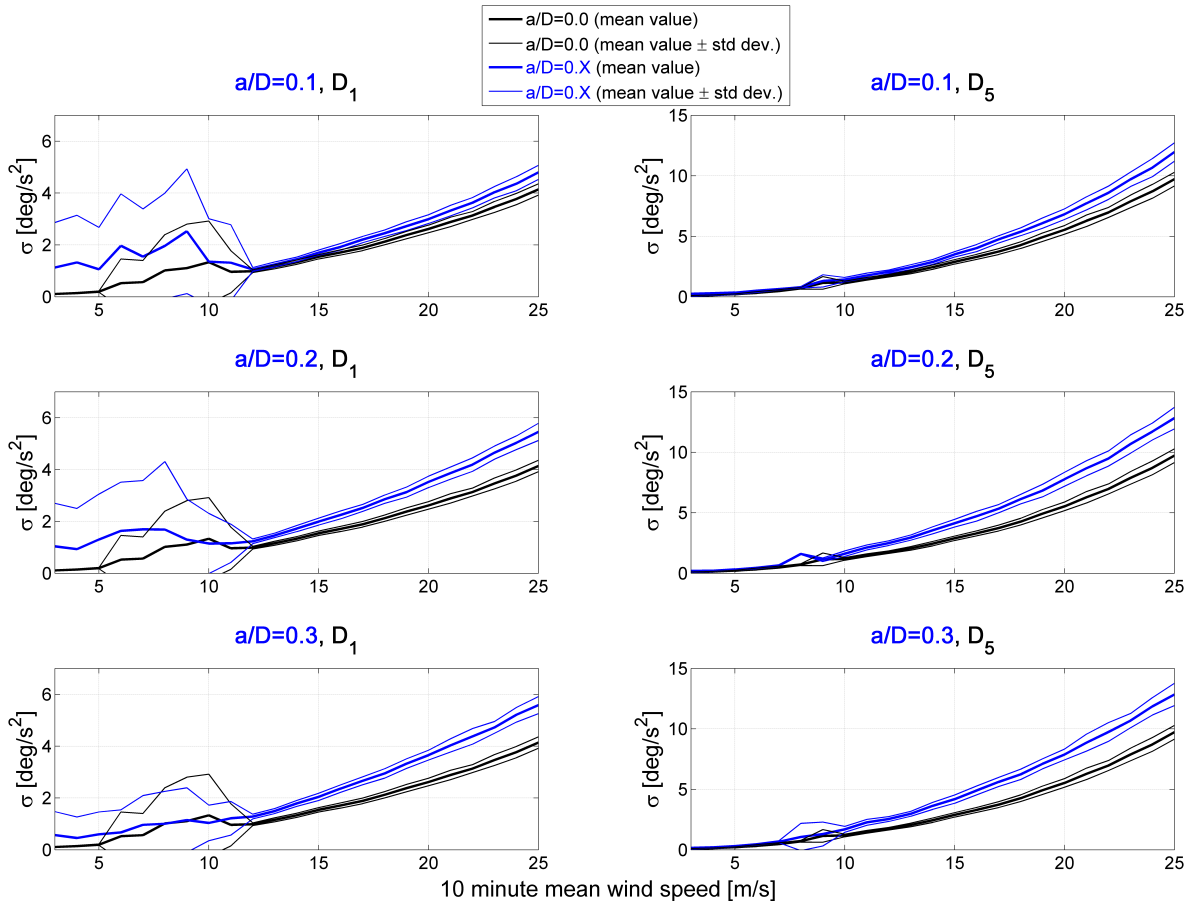

Figure 5.11: Standard deviation σ of the wavelet coefficients of the LSS rotational acceleration time series for Wavelet coefficients of levels 1 and 5 dependent on the 10-minute mean wind speeds and the crack depth a and main shaft diameter D ratio. std dev.: standard deviation.

using for averaging is performed.
Figure 5.12 shows the TSA results of LSS accelerations for different numbers of considered full rotations as well as different wind speeds dependent on the rotational position of the LSS. The number of considered full rotations is desired to be kept as low as possible in order to keep the analyzed data and data transfer as low as possible as well as to guarantee realtime condition monitoring. The lowest rotational speed of the considered 5MW NREL wind turbine is around 6.9 rpm. When considering 50 full rotations, it can take more than 7 minutes to get one measurement. But on the other hand a low number of considered rotations per measurement increases the statistical uncertainty. As seen in Figure 5.12, the spreading of the data when using 10 rotations (n=10) is largest and smallest for n=50. The difference between 20 rotations and 50 rotations is small. Therefore, in this example the number of full rotations considered is set equal to 20.
Figure 5.13 shows TSA results of different parameters for the undamaged case (a/D=0.0) and a heavily damaged

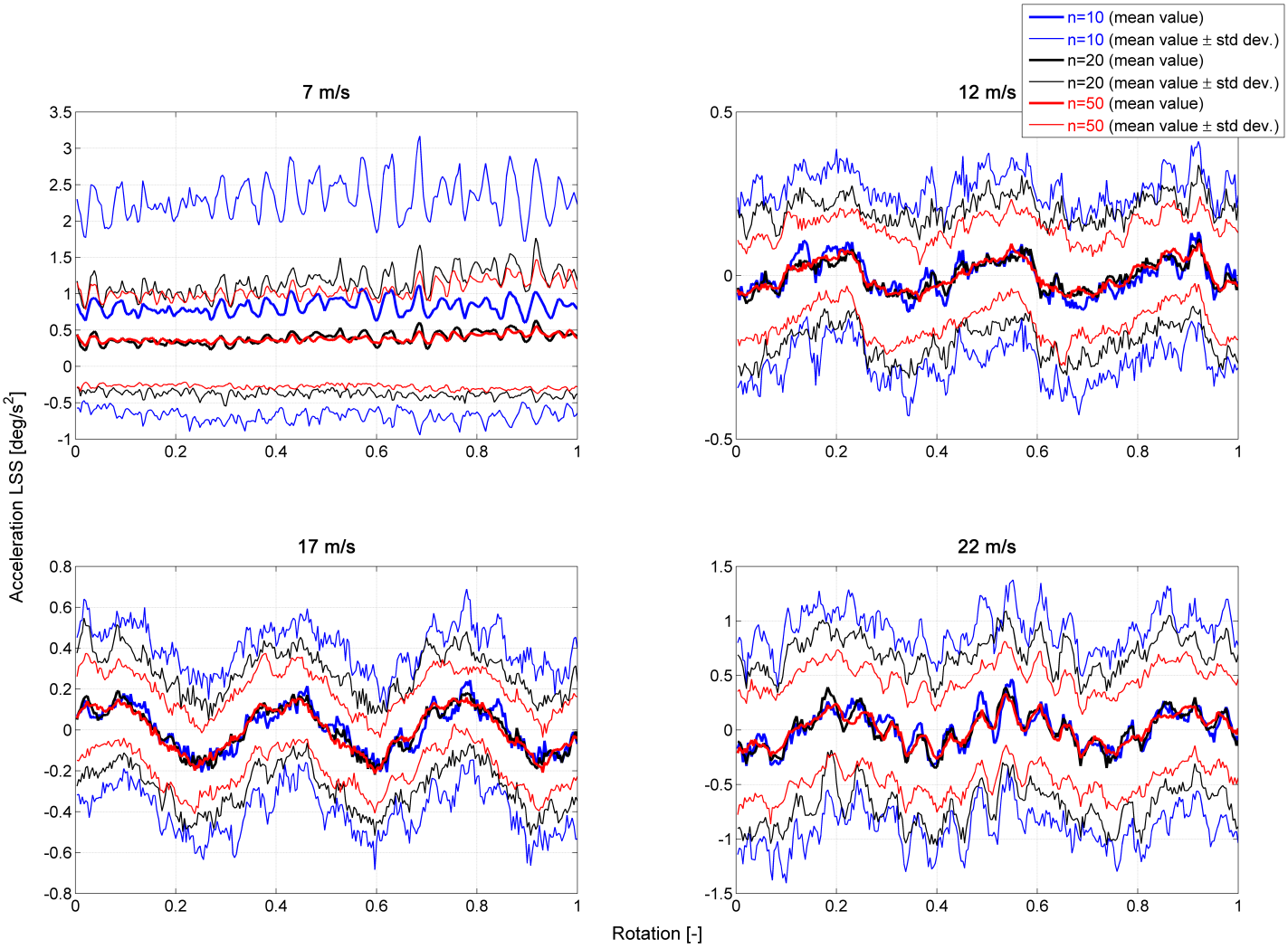

Figure 5.12: Time Synchronous Averaging (TSA) of the LSS rotational acceleration for different 10-minute wind speeds at a crack depth a and main shaft diameter D ratio of 0.1. n: number of considered full rotations of the LSS main shaft for one measurement.

LSS main shaft with a/D=0.3. From these results, the conclusion is that there are other condition monitoring strategies and analysis tools like descriptive statistics or FFT methods which give better results than TSA in this example.
But it has to mentioned that Time Synchronous Averaging has limited applicability in this example as the crack in the main shaft is not directly modeled, but adaption of the torsional stiffness of the main shaft is considered in the FAST simulations. Therefore, including the exact position of the crack on the LSS and modeling the crack in more details based on different local main shaft characteristics instead of adapting the overall torsional stiffness of the main shaft would make the TSA a more promising tool for crack detections on the main shaft as it is presented in

this example.

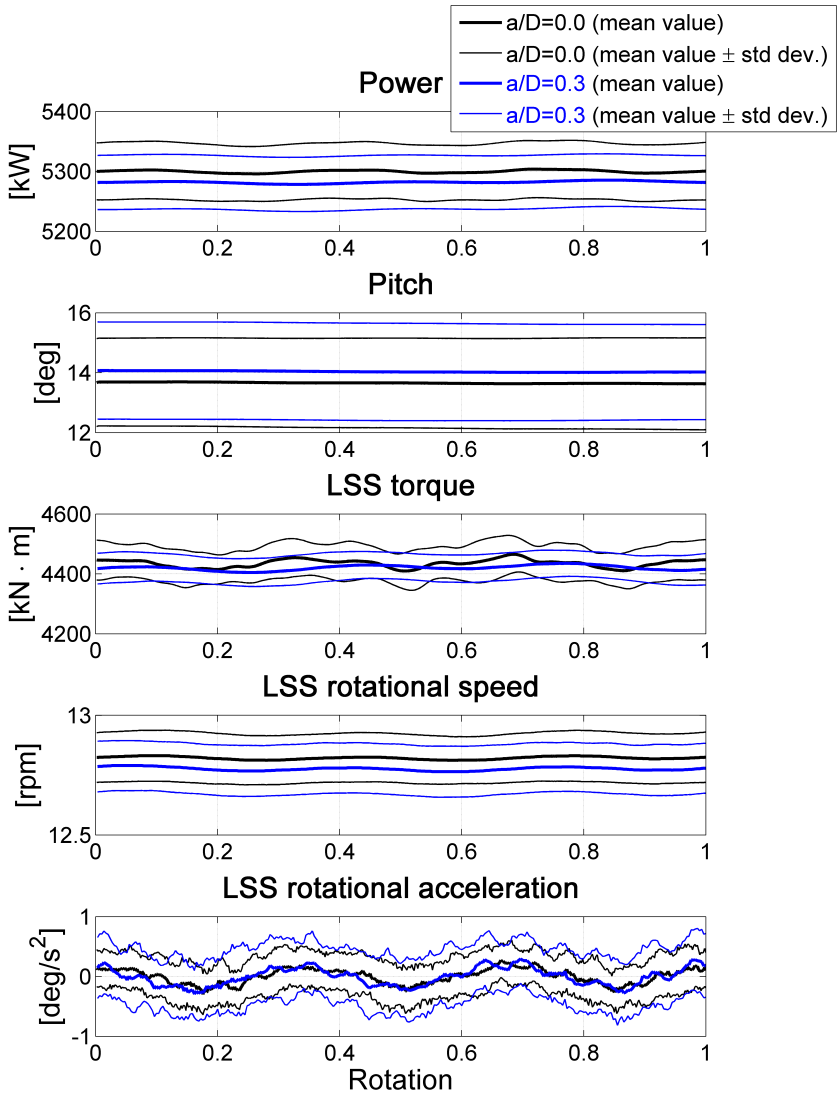

Figure 5.13: Time Synchronous Averaging (TSA) results for different parameters and different crack sizes (a/D=0.0 and a/D=0.3). The considered 10-minute mean wind speed is equal to 17 m/s and the number of considered full rotations (n) is equal to 20.

Chapter 6

Conclusions

This report focuses on different approaches in order to perform condition monitoring of the low speed shaft of an offshore wind turbine. Condition monitoring is especially important to offshore wind turbines due to their limited accessability as well as the commonly heavier and larger installed components offshore compared with wind turbines mounted onshore. Compared with other technologies in which condition monitoring is already performed, wind turbines have the problem that they are operating under varying conditions, like different rotational speeds, different wind speeds, and different turbulence intensities. These conditions lead to non-stationary conditions and make condition monitoring complex and challenging.
Different condition monitoring tools used today like simple descriptive statistics, Fast Fourier Transformations, Wavelet Transformations, Modal Assurance Criteria and Time Synchronous Averaging are investigated based on an example in order to check the applicability of these tools to detect cracks in the main shaft. The considered example in this report is based on simulations using the FAST tool. Different crack sizes are modeled and included in FAST simulations by adapting the properties of the main shaft. A stochastic model is included in order to account for uncertainties related with the simple crack model and the environmental conditions like wind speed, turbulence intensity or wave conditions.
The investigations performed in this report showed that the fluctuation of the acceleration of the low speed shaft of a wind turbine is a potential promising parameter to detect possible cracks in the main shaft. Many condition monitoring tools showed that crack detection can only be reliably performed when the actual wind speed is above rated wind speed. For lower wind speeds, the uncertainty of the compared parameter indicating a crack is often too large. The investigations showed that a crack depth equal to or larger than 20% of the main shaft diameter can be reliably detected using the considered condition monitoring approaches. This report shows that preventive maintenance planning based on condition monitoring system for crack evolution detection at the main shaft is possible.
Due to the fact that simulated data is used in order to find suitable condition monitoring methods, the proposed methods also needs to be tested under real conditions. Future work should consider more detailed modeling of the low speed shaft crack based on direct modeling of the crack instead of adapting the global characteristics of the main shaft. Studies should also include focus on the crack evolution in order to estimate the risk of collapse given a certain crack size as well as the remaining useful life (RUL).
Furthermore, the study performed in this report did not take into account any additional safety systems. In practice, safety systems could be used to stop the machine before the main shaft gets broken. Many condition monitoring procedures record parameters over time. Change over time can also be monitored and considered in condition monitoring applications. When the crack is growing fast, this issue is important.

Bibliography

[1] D. Adams, J. White, M. Rumsey, and C. Farrar. Structural health monitoring of wind turbines: method and application to a hawt. *Wind Energy*, 14(4):603–623, 2011.

[2] R. Ahmad and S. Kamaruddin. An overview of time-based and condition-based maintenance in industrial application. *Computers & Industrial Engineering*, 63(1):135 – 149, 2012.

[3] R. J. Allemang. The modal assurance criterion - twenty years of use and abuse. *Journal of Sound and Vibration*, 37:14–21, 2003.

[4] Y. Amirat, M. Benbouzid, E. Al-Ahmar, B. Bensaker, and S. Turri. A brief status on condition monitoring and fault diagnosis in wind energy conversion systems. *Renewable and Sustainable Energy Reviews*, 13(9):2629 – 2636, 2009.

[5] A. Ang and W. Tang. *Probability Concepts in Engineering: Emphasis on Applications to Civil and Environmental Engineering*. Wiley, 2007.

[6] I. Antoniadou, N. Dervilis, E. Papatheou, A. E. Maguire, and K. Worden. Aspects of structural health and condition monitoring of offshore wind turbines. *Philosophical Transactions of the Royal Society of London A: Mathematical, Physical and Engineering Sciences*, 373(2035), 2015.

[7] N. Bachschmid, P. Pennacchi, and E. Tanzi. *Cracked Rotors: A Survey on Static and Dynamic Behaviour Including Modelling and Diagnosis*. Springer Berlin Heidelberg, 2010.

[8] E. Bechhoefer and M. Kingsley. A review of time synchronous average algorithms. *Annual Conference of the Prognostics and Health Management Society, San Diego, CA, Sept*, pages 24–33, 2009.

[9] H. Braam and L. W. M. M. Rademakers. Models to analyse operation and maintenance aspects of offshore wind farm, 2004. ECN report.

[10] Brüel & Kjær Vibro GmbH. `http://www.bkvibro.com/home.html`. Available online.

[11] E. P. Carden and P. Fanning. Vibration based condition monitoring: A review. *Structural Health Monitoring*, 3(4):355–377, 2004.

[12] C. F. Christensen and T. Arnbjerg-Nielsen. Return period for environmental loads - combination of wind and wave loads for offshore wind turbines, 2000. Rambøll, Denmark.

[13] C. K. Chui. *An Introduction to Wavelets*. Academic Press Professional, Inc., San Diego, CA, USA, 1992.

[14] D. Coronado and K. Fischer. Condition Monitoring of Wind Turbines: State of the Art, User Experience and Recommendations, 2015. Project Report, IWES, Fraunhofer, Germany.

[15] David L. Laino. AeroDyn User's Guide, Version 12.50, 2002. Technical report,Windward Engineering, Salt Lake City, USA.

[16] R. R. de la Hermosa Gonzalez-Carrato, F. P. G. Marquez, and V. Dimlaye. Maintenance management of wind turbines structures via MFCs and wavelet transforms. *Renewable and Sustainable Energy Reviews*, 48:472 – 482, 2015.

[17] DNV-OS-J101. Design of offshore wind turbine structures, 2011. Det Norske Veritas, Høvik, Norway.

[18] DNV-RP-C205. Environmental conditions and environmental loads, 2010. Det Norske Veritas, Høvik, Norway.

[19] ELFORSK. Damage prevention for wind turbines - Phase 2 - Recommended measures, 2011. Elforsk report 18:11.

[20] EWEA 2015. The European offshore wind industry - key trends and statistics 2014, 2015. Euopean Wind Energy Association, January 2015.

[21] D. Ewins. *Modal testing: theory and practice*. Mechanical engineering research studies: Engineering dynamics series. Research Studies Press, 1984.

[22] FAG Industrial Services GmbH. WiPro S. `http://www.fag.de/content.fag.de/en/`. Available online.

[23] GL Garrad Hassan. Offshore wind - Operations & Maintenance opportunities in Scotland - An insight into opportunities for Scottish ports and the O&M chain, 2013. Scottish Enterprise and GL Garrad Hassan.

[24] Gram & Juhl A/S. `http://gramjuhl.com/`. Available online.

[25] Z. Hameed, Y. Hong, Y. Cho, S. Ahn, and C. Song. Condition monitoring and fault detection of wind turbines and related algorithms: A review. *Renewable and Sustainable Energy Reviews*, 13(1):1 – 39, 2009.

[26] IEC 61400-1. Wind turbines - part 1: design requirements, 2005. International Electrotechnical Comission (IEC), Geneva, Switzerland.

[27] IEC 61400-3. Wind turbines - part 3: Design requirements for offshore wind turbines, 2009. International Electrotechnical Comission (IEC), Geneva, Switzerland.

[28] International Energy Agency (IEA). Technology Roadmap: Wind energy - 2014 edition, 2013. Paris, France.

[29] ISO 10816-21. Mechanical vibration - evaluation of machine vibration by measurements on no-rotating parts - part 21: Onshore wind turbines with gearbox.

[30] A. K. Jardine, D. Lin, and D. Banjevic. A review on machinery diagnostics and prognostics implementing condition-based maintenance. *Mechanical Systems and Signal Processing*, 20(7):1483 – 1510, 2006.

[31] Jason M. Jonkman and M. L. Buhl. FAST User's Guide, 2005. National Renewable Energy Laboratory (NREL), Technical report, NREL/EL-500-38230.

[32] Jason M. Jonkman and S. Butterfield and W. Musial and G. Scott. Definition of a 5MW Reference Wind Turbine for Offshore System Development, 2009. National Renewable Energy Laboratory (NREL), Technical report, NREL/EL-500-38060.

[33] JCSS. Probabilistic model code. `http://www.jcss.byg.dtu.dk`, 2001. Joint Committee on Structural Safety.

[34] P. G. Kulkarni and A. D. Sahasrabudhe. Application of wavelet transform for fault diagnosis of rolling element bearings. *International Journal of Scientific and Technology Research*, 2(4):138 – 148, 2013.

[35] C. J. Lissenden, S. P. Tissot, M. W. Trethewey, and K. P. Maynard. Torsion response of a cracked stainless steel shaft. *Fatigue & Fracture of Engineering Materials & Structures*, 30(8):734–747, 2007.

[36] W. Liu, B. Tang, J. Han, X. Lu, N. Hu, and Z. He. The structure healthy condition monitoring and fault diagnosis methods in wind turbines: A review. *Renewable and Sustainable Energy Reviews*, 44(0):466 – 472, 2015.

[37] B. Lu, Y. Li, X. Wu, and Z. Yang. A review of recent advances in wind turbine condition monitoring and fault diagnosis. In *Power Electronics and Machines in Wind Applications (PEMWA)*, pages 1–7, June 2009.

[38] M. Brogan. Making sense of the CMS market. http://www.windsystemsmag.com/article/detail/483/making-sense-of-the-cms-market. Wind Systems Magazine April 2013.

[39] F. P. G. Marquez, A. M. Tobias, J. M. P. Perez, and M. Papaelias. Condition monitoring of wind turbines: Techniques and methods. *Renewable Energy*, 46(0):169 – 178, 2012.

[40] Y. Meyer and R. Ryan. *Wavelets: Algorithms and Applications*. Society for Industrial and Applied Mathematics (SIAM), Philadelphia, USA, 1993.

[41] Mita-Teknik. MiCMS^{TM}Condition Monitoring System. `http://www.mita-teknik.com/solutions/condition-monitoring/`. Available online.

[42] P. J. Moriarty and A. C. Hansen. AeroDyn Theory Manual, 2005. National Renewable Energy Laboratory (NREL), Technical report, NREL/TP-500-36881.

[43] Z. Peng and F. Chu. Application of the wavelet transform in machine condition monitoring and fault diagnostics: a review with bibliography. *Mechanical Systems and Signal Processing*, 18(2):199 – 221, 2004.

[44] PRÜFTECHNIK Dieter Busch AG. Online Condition Monitoring Systems. `http://www.pruftechnik.com/products/condition-monitoring-systems`. Available online.

[45] REN21. Renewables 2015: Global status report, 2015. Paris, France.

[46] J. Sanz, R. Perera, and C. Huerta. Gear dynamics monitoring using discrete wavelet transformation and multi-layer perceptron neural networks. *Applied Soft Computing*, 12(9):2867 – 2878, 2012.

[47] C. Sheng, Z. Li, L. Qin, Z. Guo, and Y. Zhang. Recent progress on mechanical condition monitoring and fault diagnosis. *Procedia Engineering*, 15(0):142 – 146, 2011.

[48] S. Sheng and P. Veers. Wind turbine drive train condition monitoring - an overview. In *Mechanical Failures Prevention Group: Applied Systems Health Management Conference 2011*, 2011. Virginia Beach, Virginia.

[49] SKF WindCon. Remote monitoring for reliable performance. `http://www.skf.com/group/industry-solutions/wind-energy/`. Available online.

[50] N. Tarp-Johansen, J. Sørensen, and P. Madsen. Experience with acceptance criteria for offshore wind turbines in extreme loading. In *Proceedings of JCSS Workshop on Reliability Based Code Calibration, Zurich, March 21-22, 2002*.

[51] P. Tchakoua, R. Wamkeue, M. Ouhrouche, F. Slaoui-Hasnaoui, T. A. Tameghe, and G. Ekemb. Wind turbine condition monitoring: State-of-the-art review, new trends, and future challenges. *Energies*, 7(4):2595, 2014.

[52] G. Vachtsevanos, F. Lewis, M. Roemer, A. Hess, and B. Wu. *Intelligent Fault Diagnosis and Prognosis for Engineering Systems*. John Wiley & Sons, Inc., 2006.

[53] G. J. W. Van Bussel and M. B. Zaaijer. Reliability, availability and maintenance aspects of large-scale offshore wind farms, a concepts study. In *International Conference on Marine Renewable Energies (MAREC)*, 2001. Newcastle, UK.

[54] T. W. Verbruggen. Wind turbine operation & maintenance based on condition monitoring - wt-ω, 2003. ECN report (ECN-C-03-047), Energy research Centre of the Netherlands (ECN),The Netherlands.

[55] J. Wheeler and W. Zurek. *Quantum Theory and Measurement*. Princeton Legacy Library. Princeton University Press, 1983.

[56] E. Wiggelinkhuizen, T. Verbruggen, H. Bram, L. Rademakers, J. Xiang, and S. J. Watson. Assessment of condition monitoring techniques for offshore wind farms. *Journal of Solar Energy Engineering*, 130(3), 2008.

[57] W. Yang, P. J. Tavner, C. J. Crabtree, Y. Feng, and Y. Qiu. Wind turbine condition monitoring: technical and commercial challenges. *Wind Energy*, 17(5):673–693, 2014.

[58] A. Zaher, S. McArthur, D. Infield, and Y. Patel. Online wind turbine fault detection through automated scada data analysis. *Wind Energy*, 12(6):574–593, 2009.

[59] Z. Zhang, Z. Yin, T. Han, and A. C. Tan. Fracture analysis of wind turbine main shaft. *Engineering Failure Analysis*, 34:129 – 139, 2013.

[60] W. Zhao, D. Siegel, J. Lee, and L. Liying. An integrated framework of drivetrain degradation assessment and fault localization for offshore wind turbines. *International Journal of Prognostics and Health Management*, 4(012):1–13, 2013.

[61] K. Zhu, Y. S. Wong, and G. S. Hong. Wavelet analysis of sensor signals for tool condition monitoring: A review and some new results. *International Journal of Machine Tools and Manufacture*, 49(7-8):537 – 553, 2009.

Different Condition Monitoring Approaches for Main Shafts of Offshore Wind Turbines

ISSN 1901-726X

DCE Technical Report No. 212